Heavy Elements in Late-Phase Spectra of Kilonovae

Implications for GW170817

Salma Rahmouni
Tohoku University

Masaomi Tanaka (Tohoku University), Kato Daiji (NIFS)

YITP long-term workshop Feb 18th, 2026

Introduction

Binary Neutron Stars

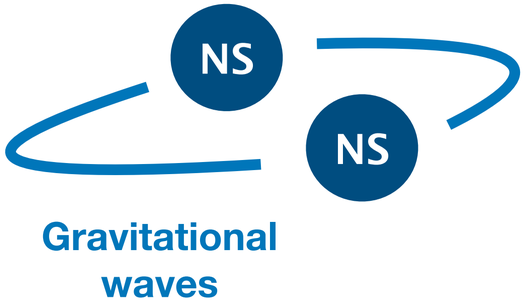

Merger

Post-merger ejecta

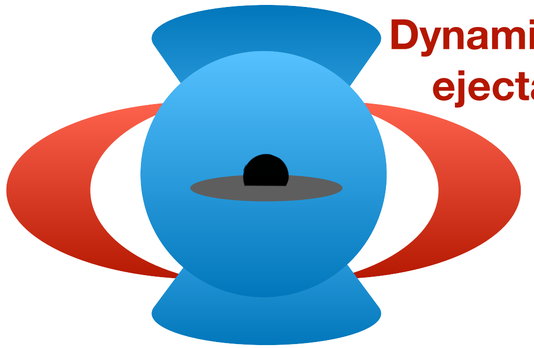

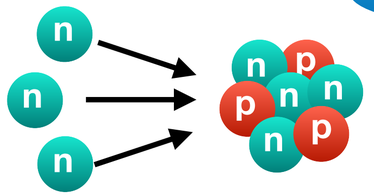

Nucleosynthesis of heavy elements by rapid neutron capture process (r-process)

Electromagnetic Emission “Kilonova"

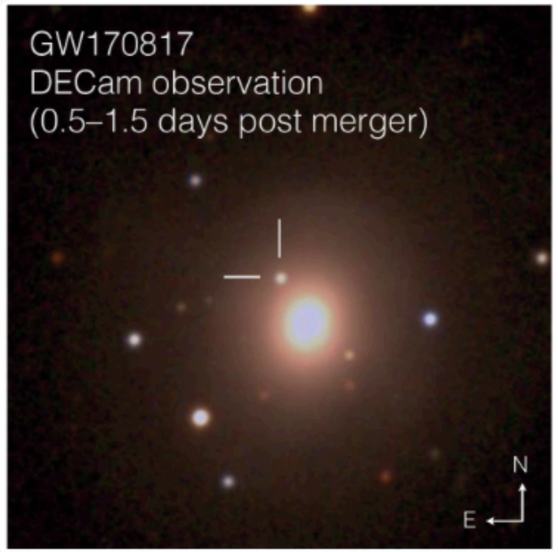

Introduction

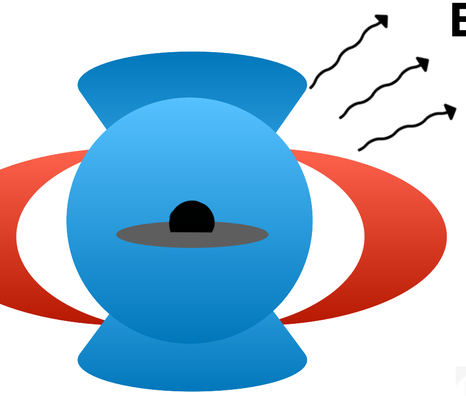

Electromagnetic emission
“Kilonova”

Kilonova of GW170817

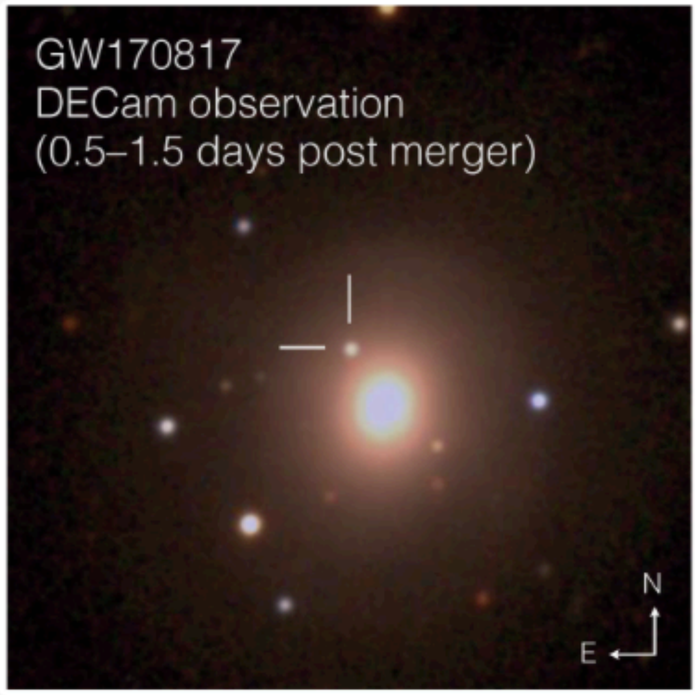

Soares-Santos et al. (2017)

GW170817 spectrum

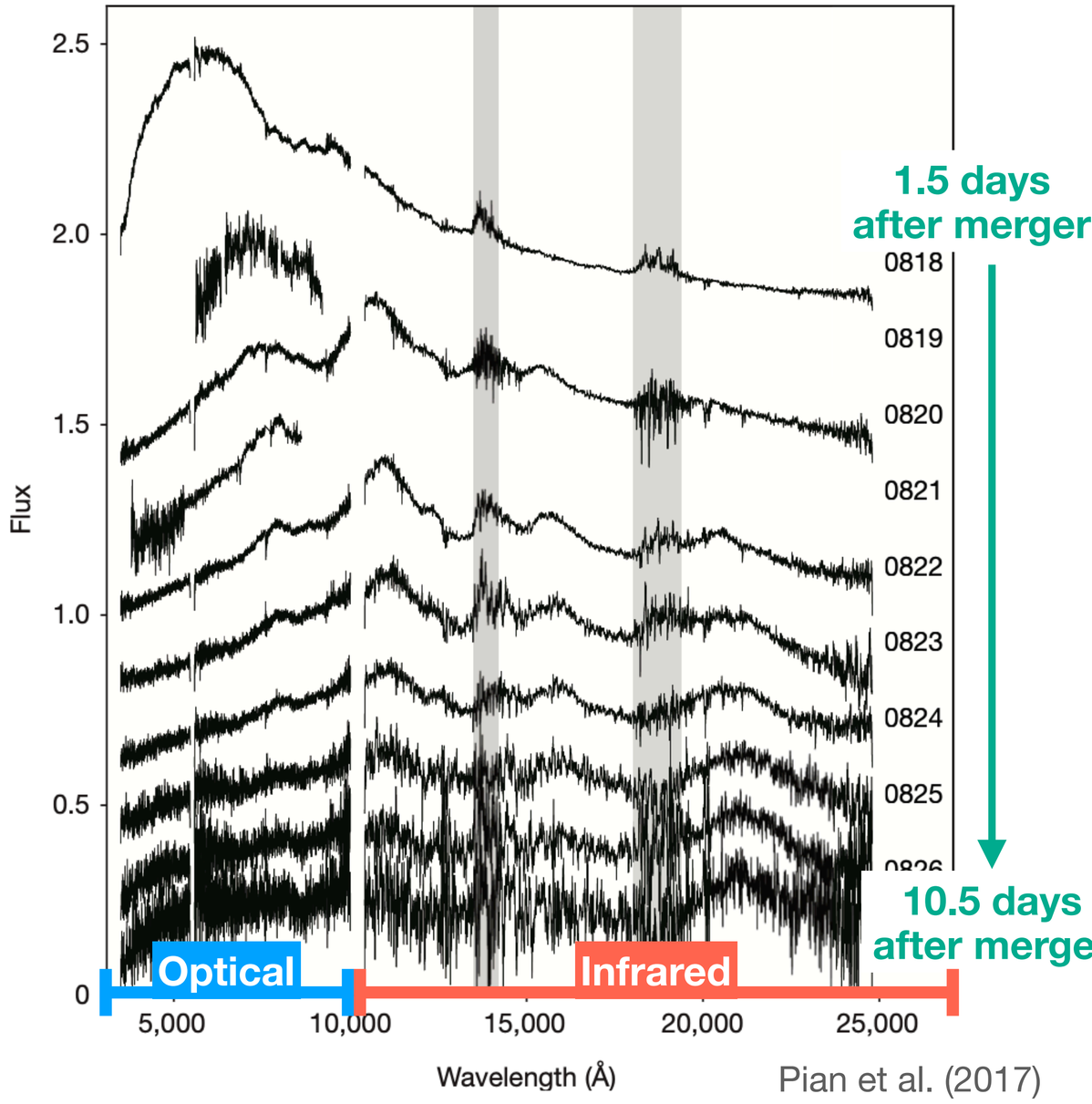

Pian et al. (2017)

Introduction

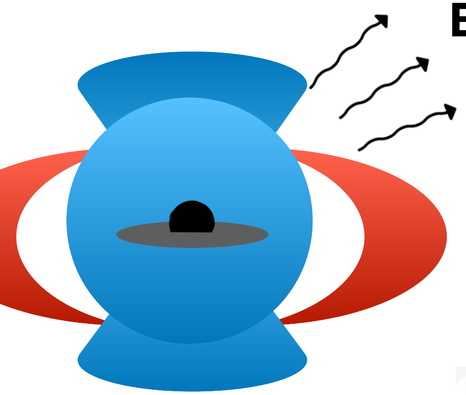

Electromagnetic emission
“Kilonova”

Kilonova of GW170817

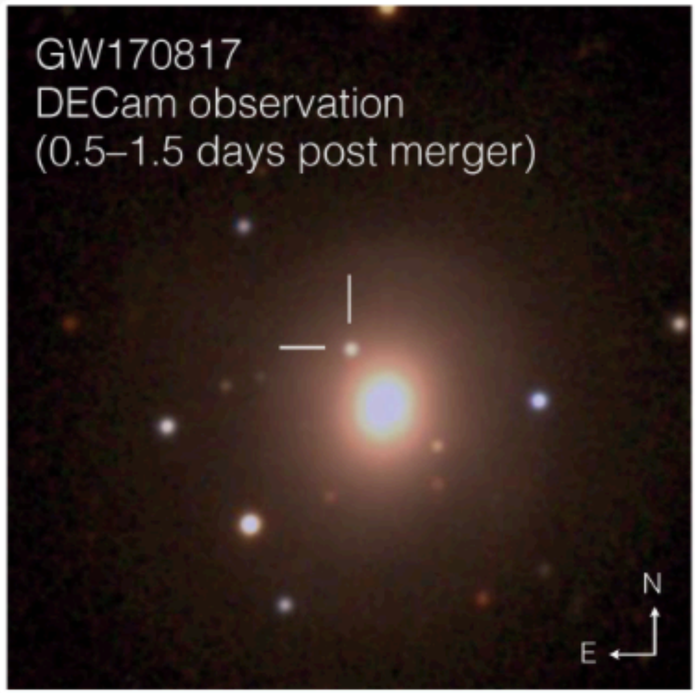

Soares-Santos et al. (2017)

GW170817 spectrum

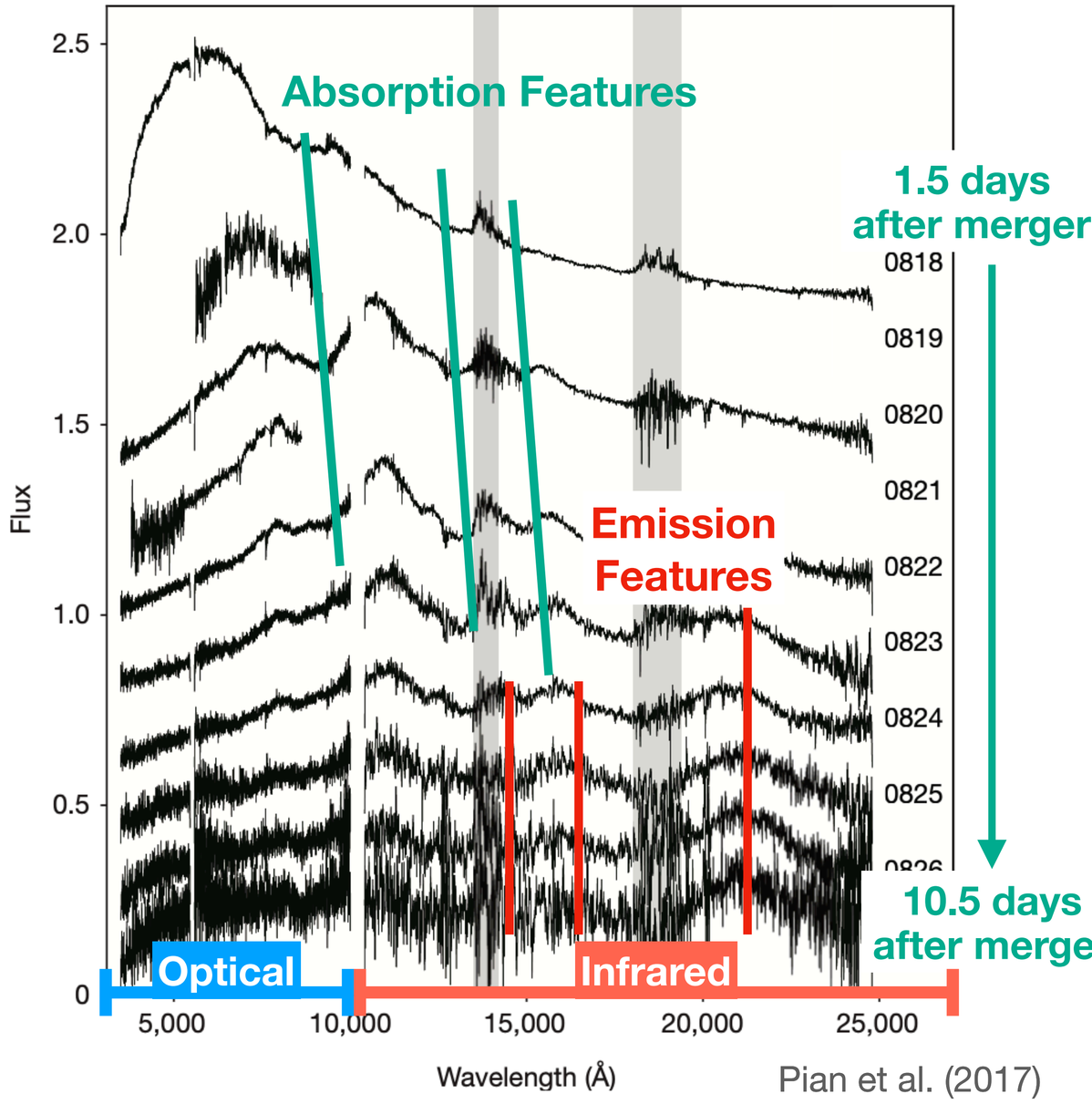

Pian et al. (2017)

Introduction

Electromagnetic emission
"Kilonova"

Goal

Quantify the mass fraction of heavy elements in NSMs to ultimately understand nucleosynthesis of heavy elements

First step: Spectral Investigation

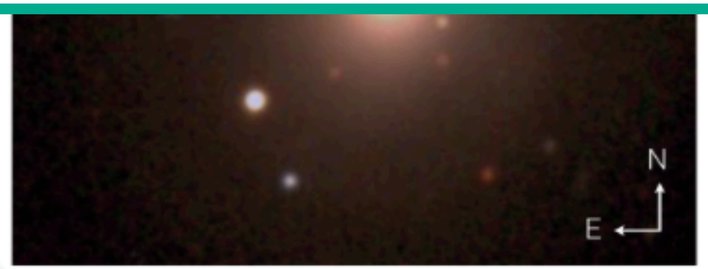

Soares-Santos et al. (2017)

GW170817 spectrum

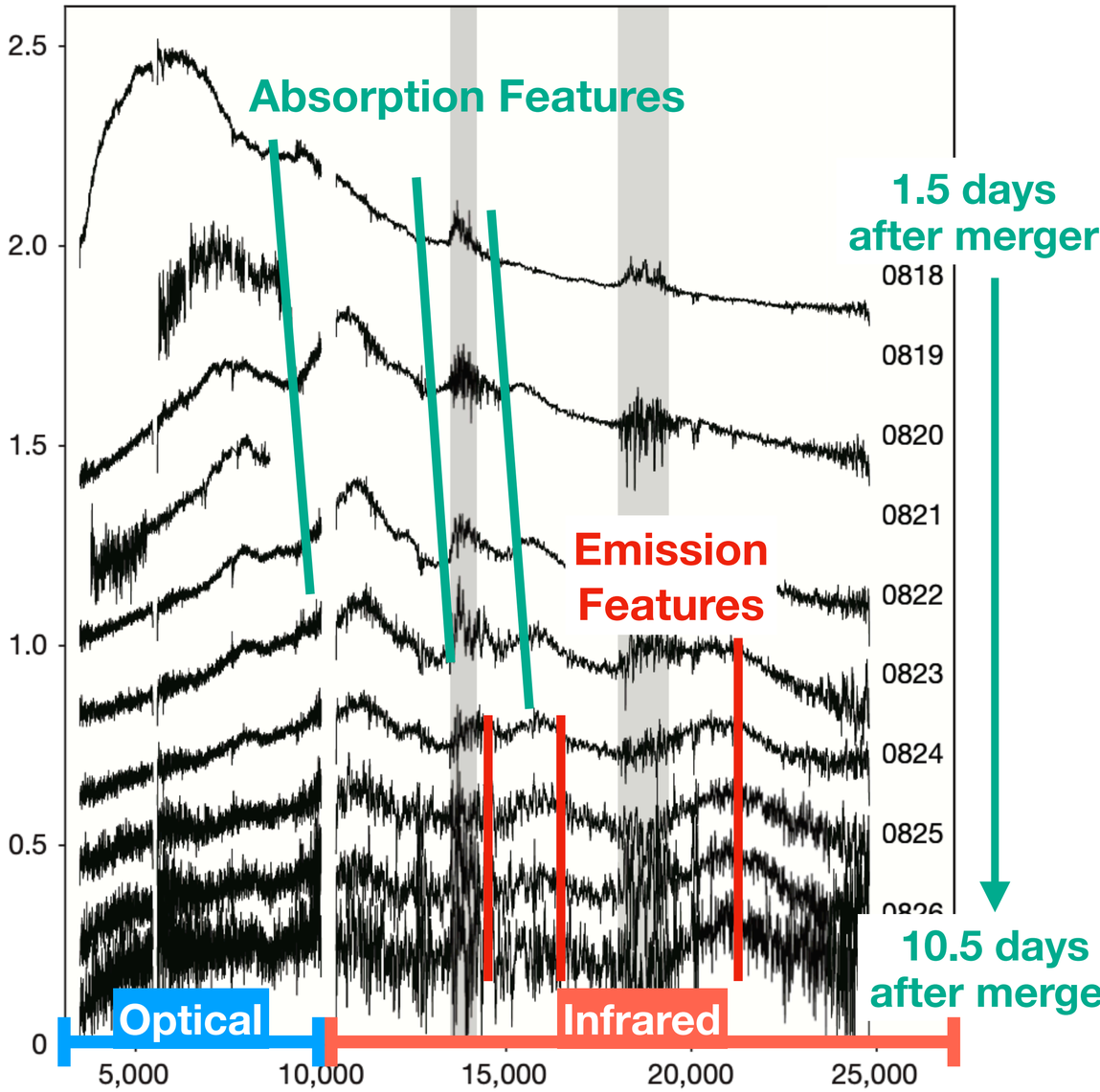

Pian et al. (2017)

Early-Phase Spectral Investigation

Identification of Most Features

(Watson+19, Domoto+22, Sneppen+23, SR+25)

1 H																	2 He
3 Li	4 Be											5 B	6 C	7 N	8 O	9 F	10 Ne
11 Na	12 Mg											13 Al	14 Si	15 P	16 S	17 Cl	18 Ar
19 K	20 Ca	21 Sc	22 Ti	23 V	24 Cr	25 Mn	26 Fe	27 Co	28 Ni	29 Cu	30 Zn	31 Ga	32 Ge	33 As	34 Se	35 Br	36 Kr
37 Rb	38 Sr	39 Y	40 Zr	41 Nb	42 Mo	43 Tc	44 Ru	45 Rh	46 Pd	47 Ag	48 Cd	49 In	50 Sn	51 Sb	52 Te	53 I	54 Xe
55 Cs	56 Ba		72 Hf	73 Ta	74 W	75 Re	76 Os	77 Ir	78 Pt	79 Au	80 Hg	81 Tl	82 Pb	83 Bi	84 Po	85 At	86 Rn
87 Fr	88 Ra		104 Rf	105 Db	106 Sg	107 Bh	108 Hs	109 Mt	110 Ds	111 Rg	112 Cn	113 Nh	114 Fl	115 Mc	116 Lc	117 Ts	118 Og
			57 La	58 Ce	59 Pr	60 Nd	61 Pm	62 Sm	63 Eu	64 Gd	65 Tb	66 Dy	67 Ho	68 Er	69 Tm	70 Yb	71 Lu
			89 Ac	90 Th	91 Pa	92 U	93 Np	94 Pu	95 Am	96 Cm	97 Bk	98 Cf	99 Es	100 Fm	101 Md	102 No	103 Lr

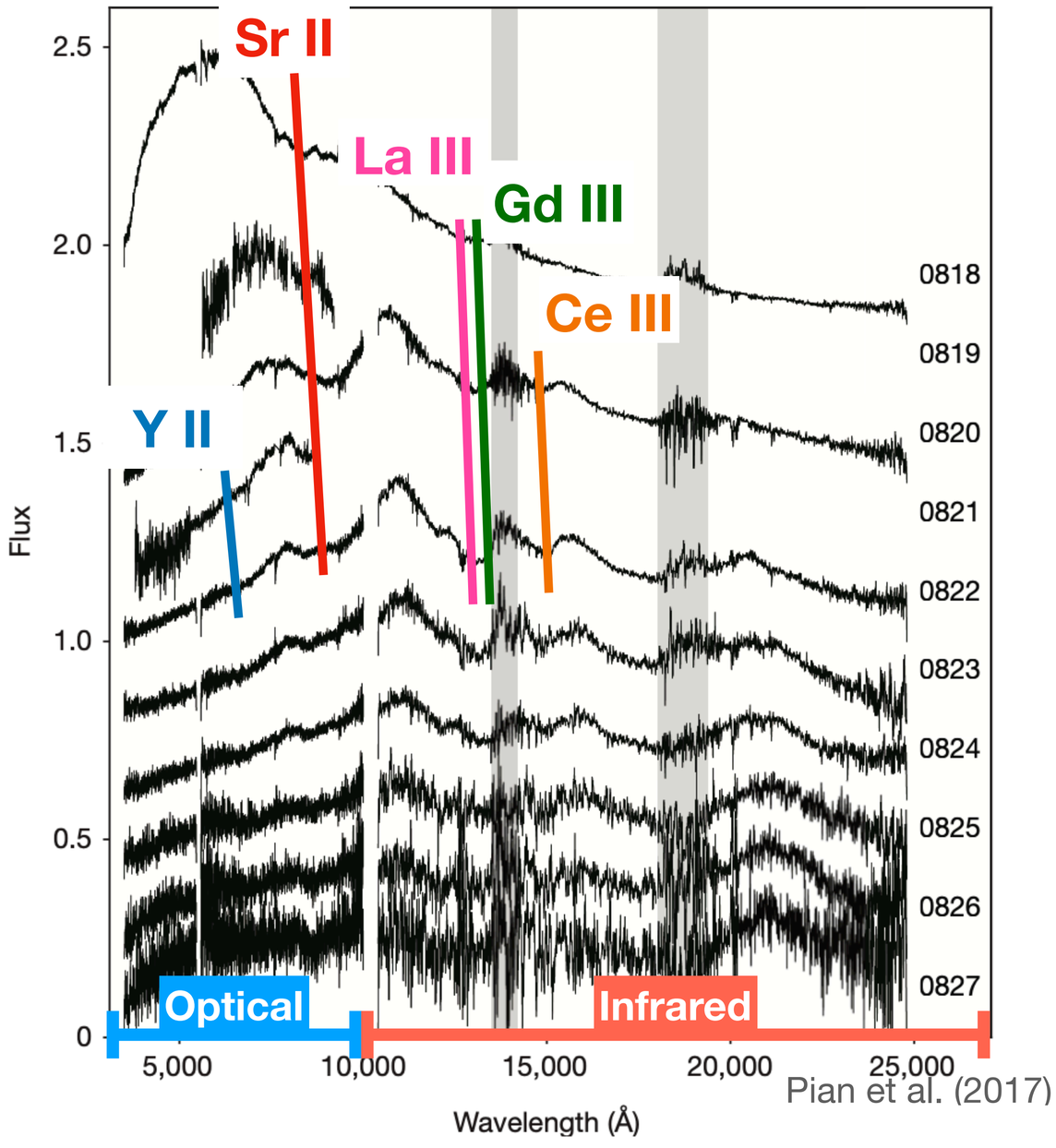

Pian et al. (2017)

Early-Phase Spectral Investigation

Identification of Most Features

(Watson+19, Domoto+22, Sneppen+23, SR+25)

Constraints on Nucleosynthesis

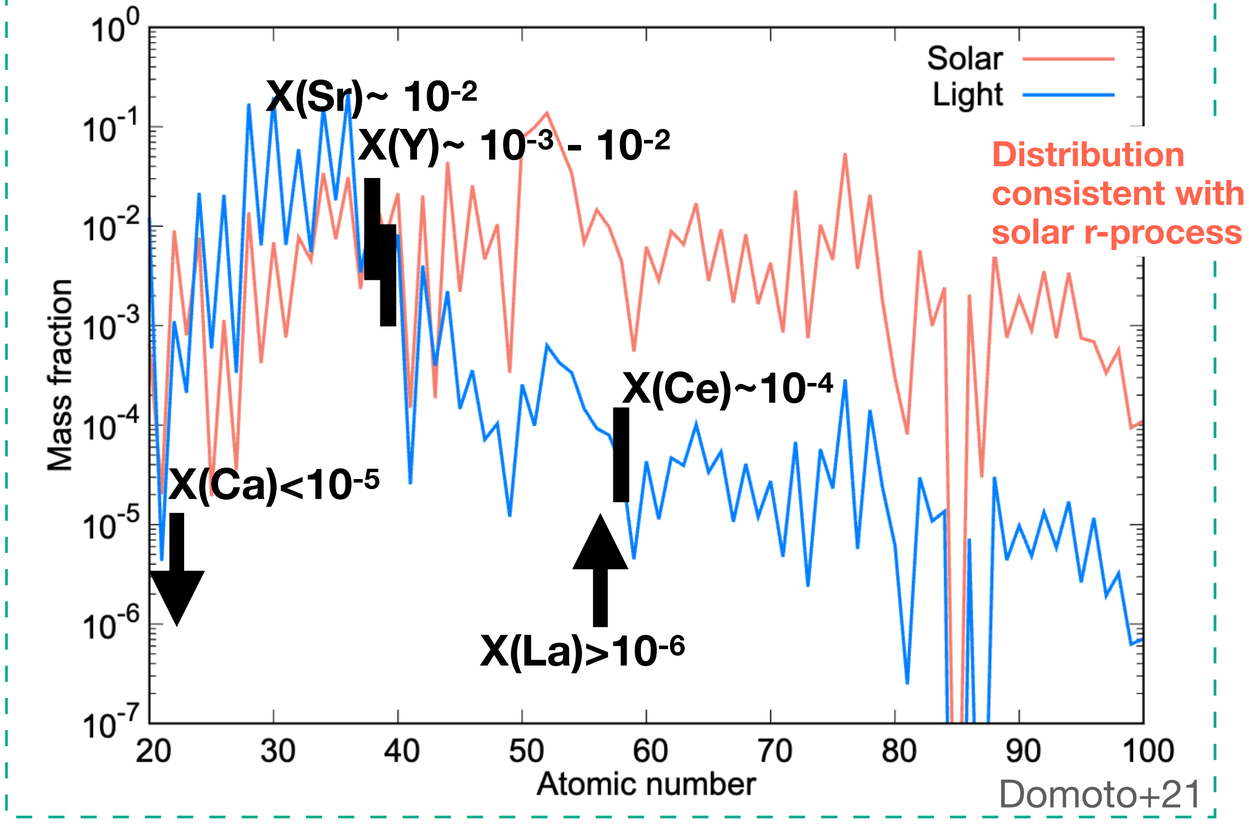

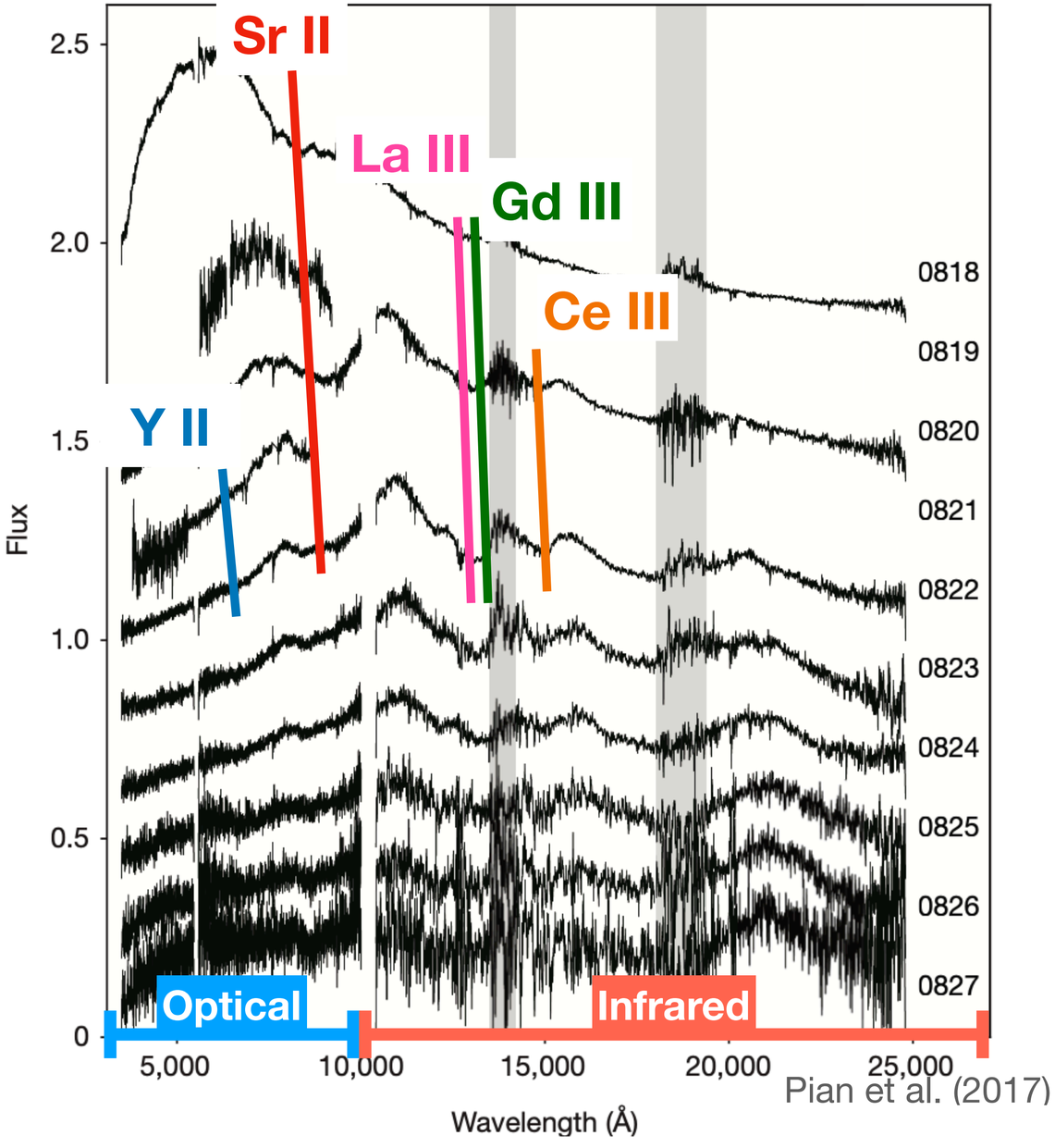

Late-Phase Spectral Investigation

Identification of a Single Feature

(Hotokezaka+23)

Constraints on Nucleosynthesis

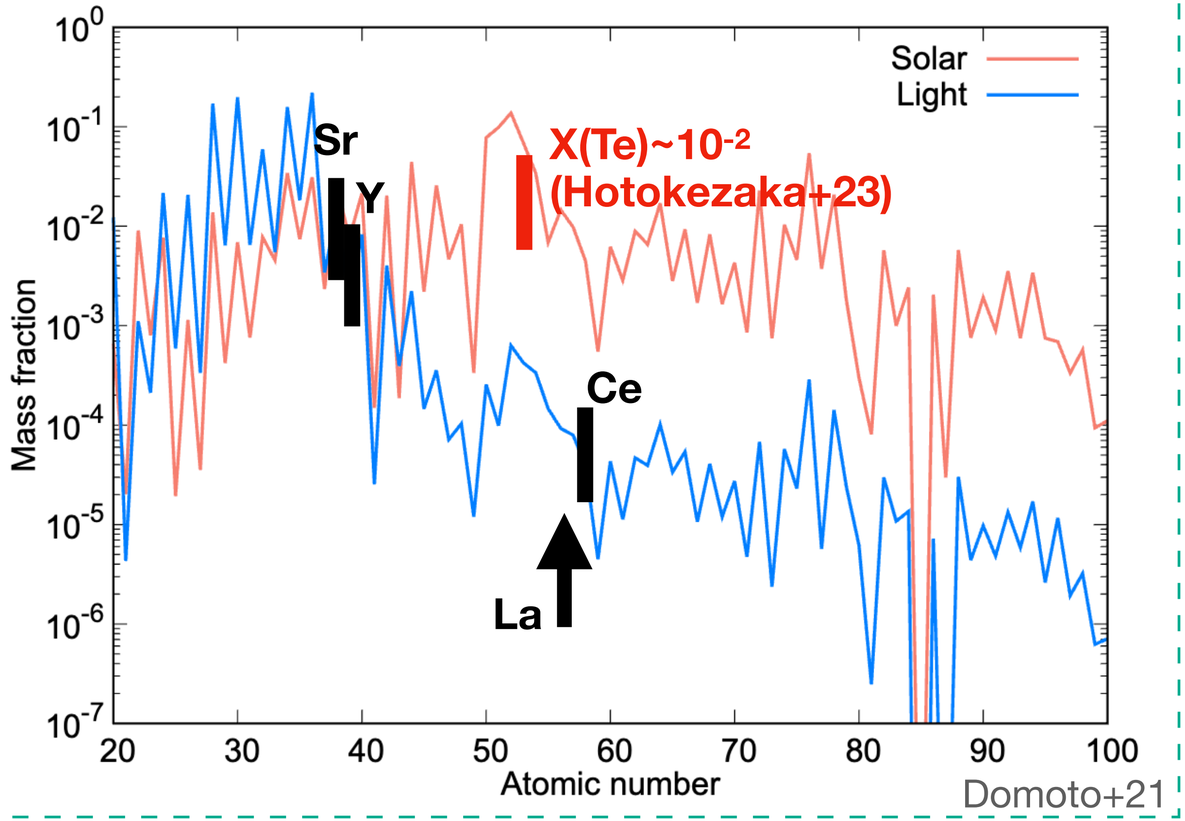

Inconsistency?

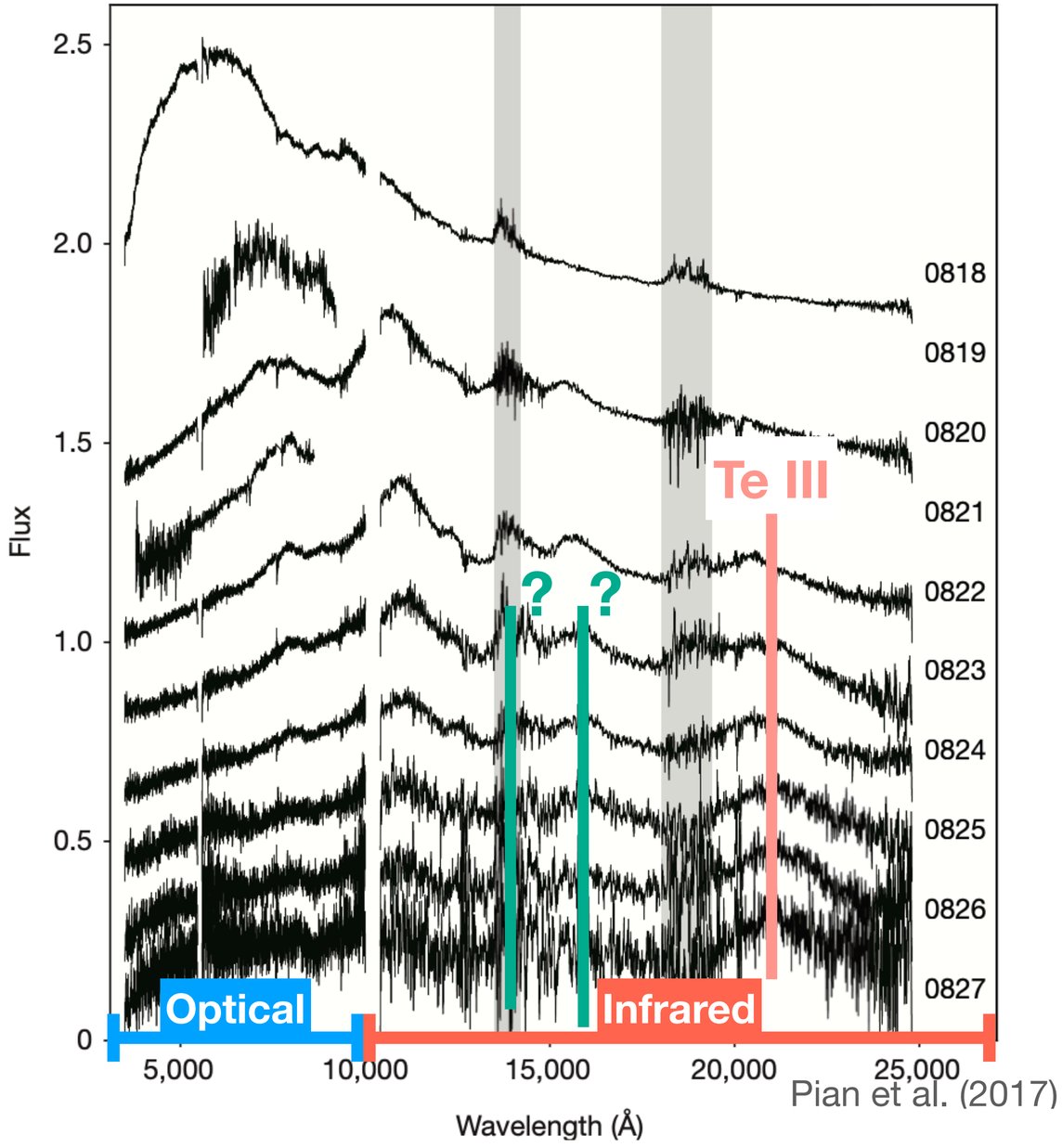

Pian et al. (2017)

Late-Phase Spectral Investigation

Notable Previous Works

Gillanders+23: Several candidates for each feature

Pognan+23, 25: non-LTE radiative transfer simulations for few selected elements

Jerkstrand+25: non-LTE simulations for weak r-process elements

No robust Identification of all late-phase features has been performed so far

This work

Comprehensive analysis using a simple spectral model including all elements to explain observed features

Spectral Model

Late-phase features are caused by radiative decay of collisionally excited elements

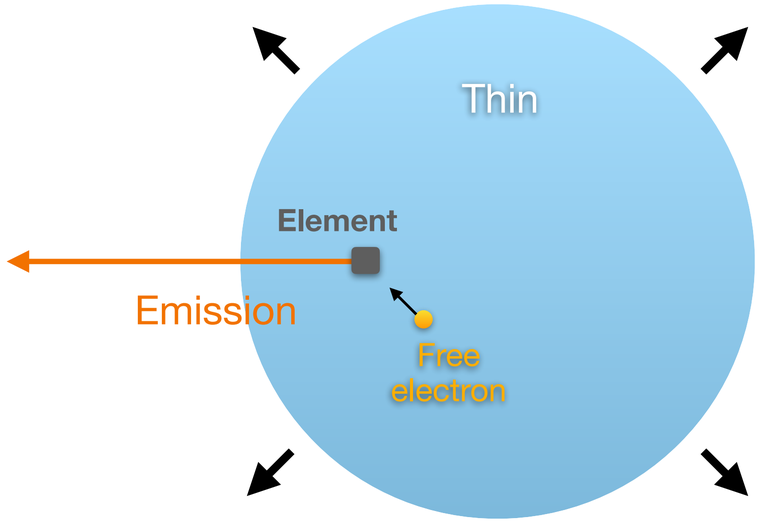

Light Elements: no mixing between configurations

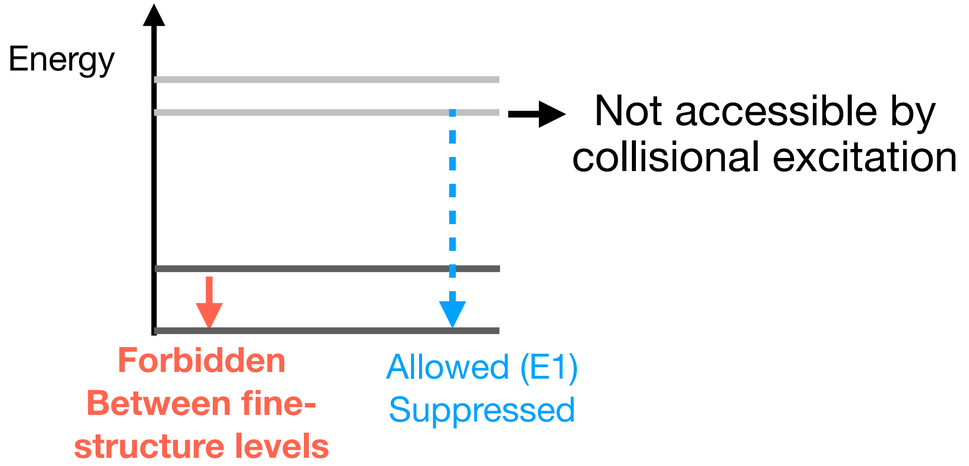

Heavy Elements: large mixing between configurations

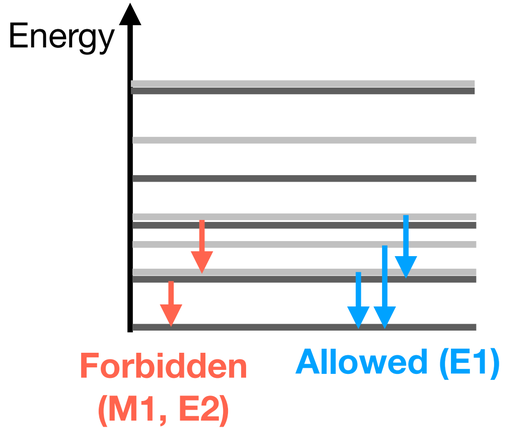

Allowed and Forbidden decays from collisional excitation are possible

Spectral Model

Emission observed at late-phase is due to collisionally excited elements

Late-phase ejecta

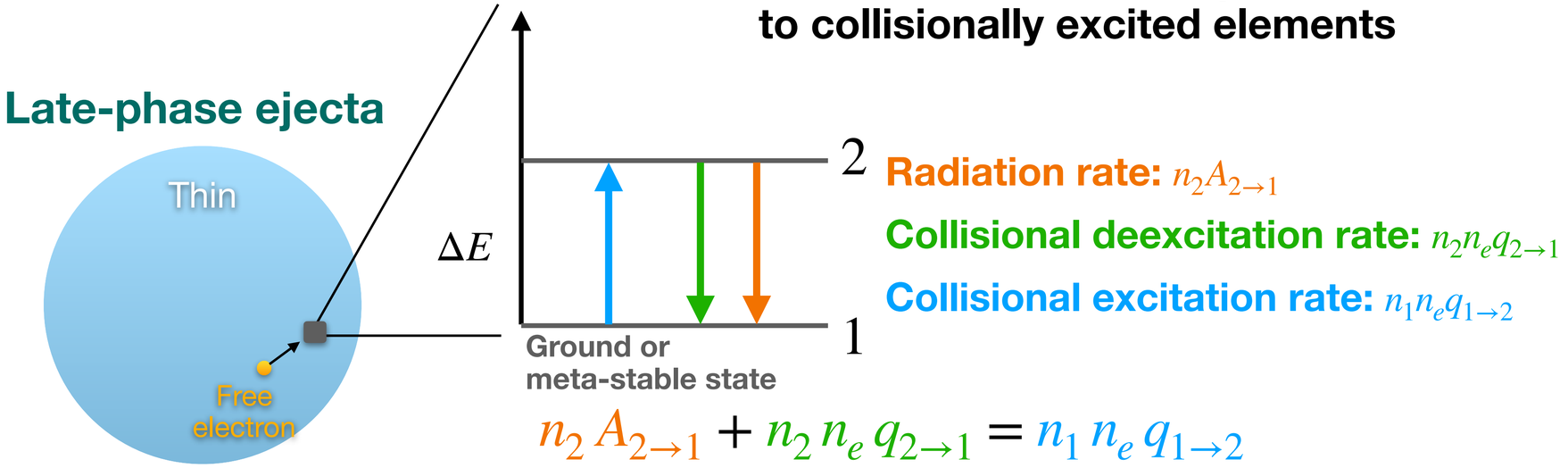

Radiation rate: $n_2 A_{2\to1}$

Collisional deexcitation rate: $n_2 n_e q_{2\to1}$

Collisional excitation rate: $n_1 n_e q_{1\to2}$

$$n_2\,A_{2\to1} + n_2\,n_e\,q_{2\to1} = n_1\,n_e\,q_{1\to2}$$

Luminosity (per volume): $L = \Delta E\, n_2\, A_{2\to1}$

Rate coefficient: (Atomic property)

$$q_{1\to2} = \frac{8.629\times10^{-6}}{T^{1/2}}\frac{\Upsilon_{1\to2}}{g_1}\exp(-\Delta E/kT_e)$$

Electron density $n_e \sim 10^7\,\mathrm{cm^{-3}}$

Electron temperature $T_e \sim 2000\,\mathrm{K}$

Einstein coefficient:

Allowed: $A_{2\to1} \sim 10^6\,\mathrm{s^{-1}}$

Forbidden: $A_{2\to1} \sim 1\,\mathrm{s^{-1}}$

Spectral Model

Emission observed at late-phase is due to collisionally excited elements

Late-phase ejecta

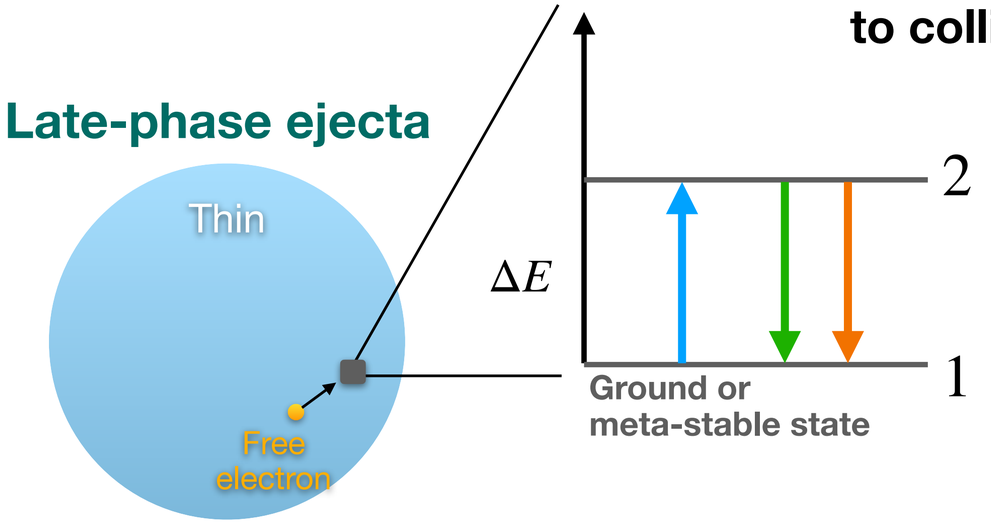

Radiation rate: $n_2 A_{2\to1}$

Collisional deexcitation rate: $n_2 n_e q_{2\to1}$

Collisional excitation rate: $n_1 n_e q_{1\to2}$

Luminosity (per volume): $L = \Delta E\, n_2\, A_{2\to1}$

Resulting Spectrum:

- Selection of forbidden and allowed transitions of all elements
- Doppler broadening of $0.07c$

Example of doubly ionized state with solar abundance

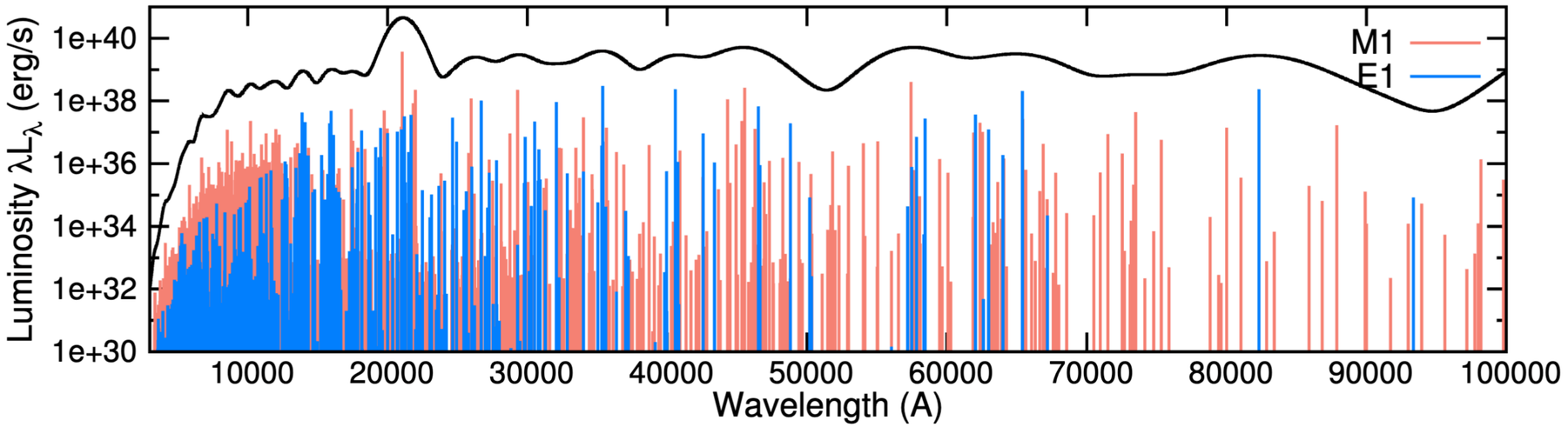

Comparison with GW170817

Assuming same abundance as in early phase

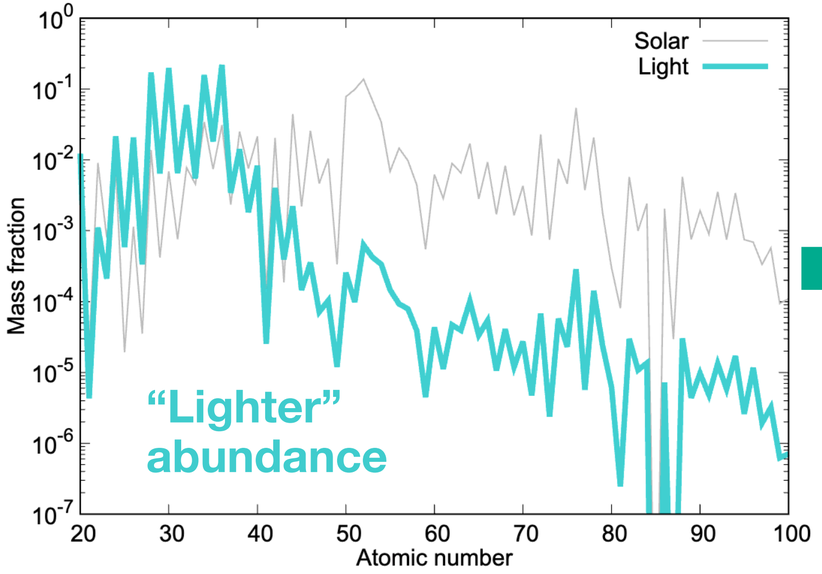

Model spectrum + Blackbody continuum compared with GW170817 observed spectrum at 9.4 days

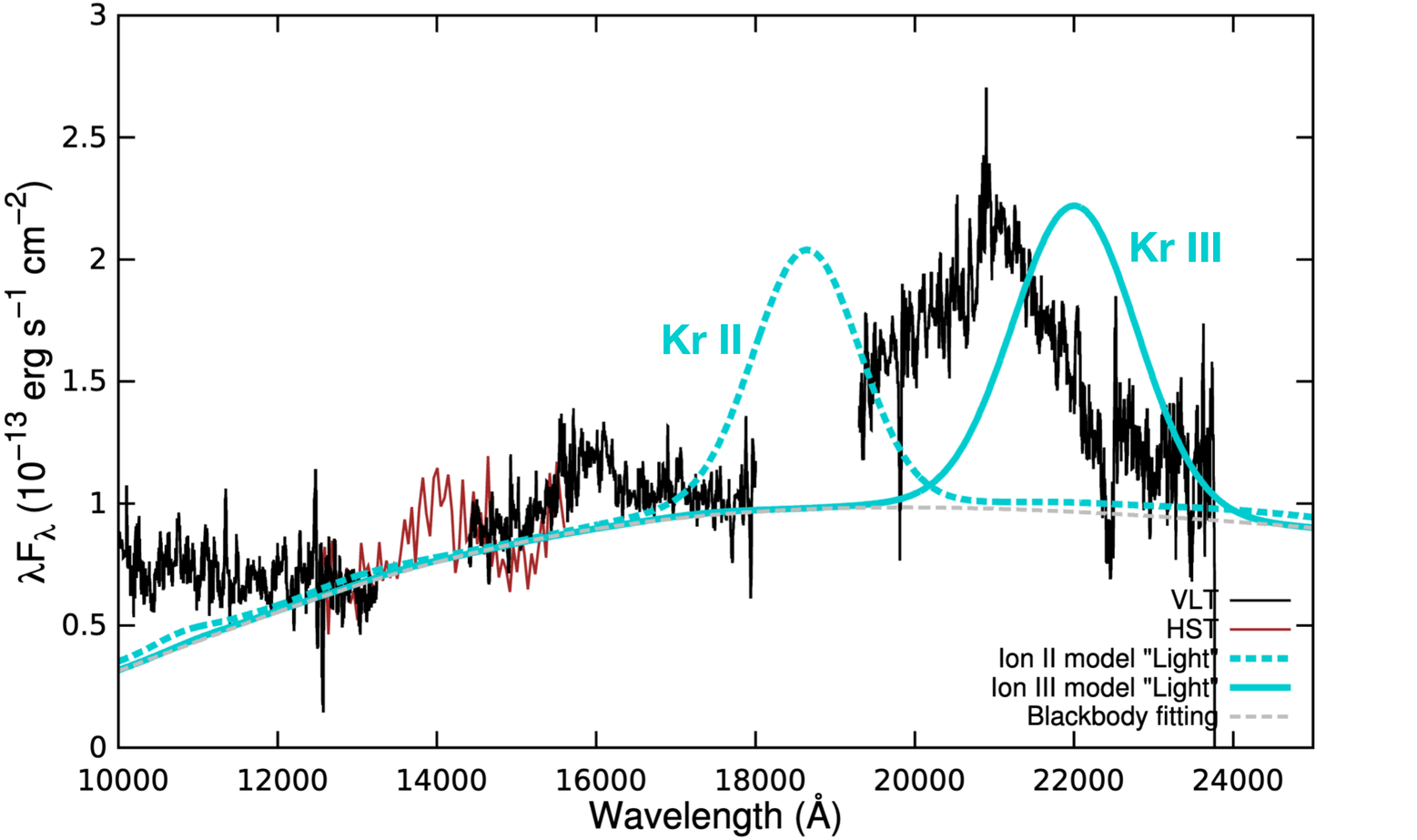

We cannot reproduce any of GW170817 late-phase features with light abundance assumption

Comparison with GW170817

Assuming abundance consistent with solar r-process

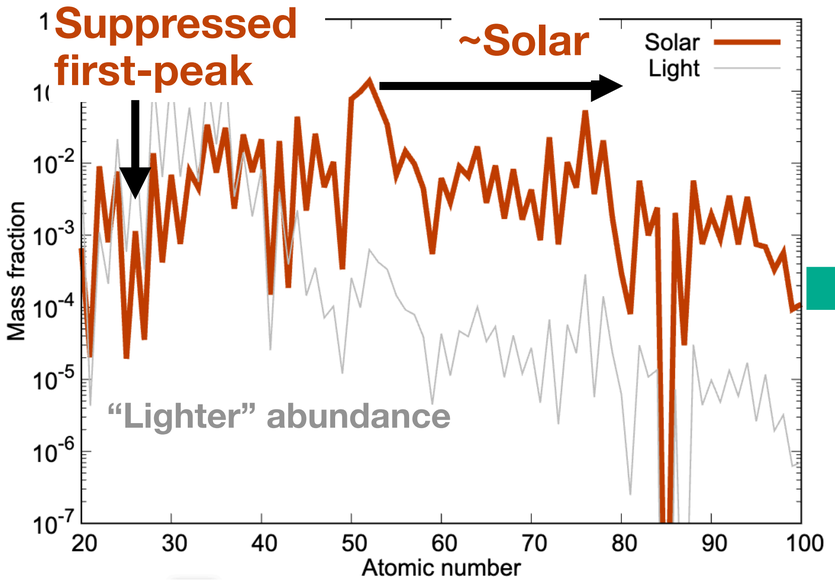

Best-fit model spectrum + Blackbody continuum with GW170817 observed spectrum at 9.4 days

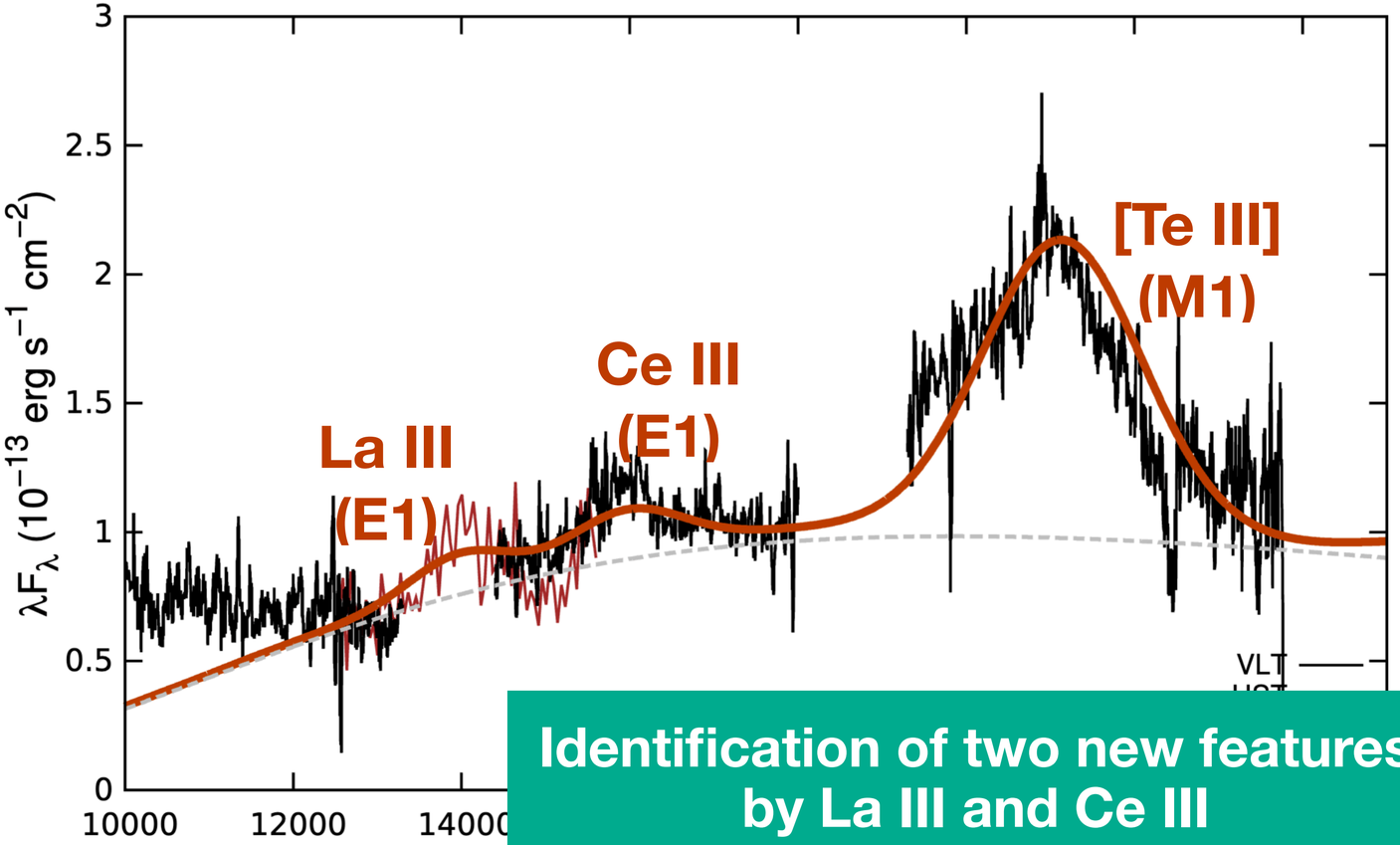

Identification of two new features by La III and Ce III + confirmation of Te III line

*Effect of other lines at each feature is not significant

Nucleosynthesis Constraints

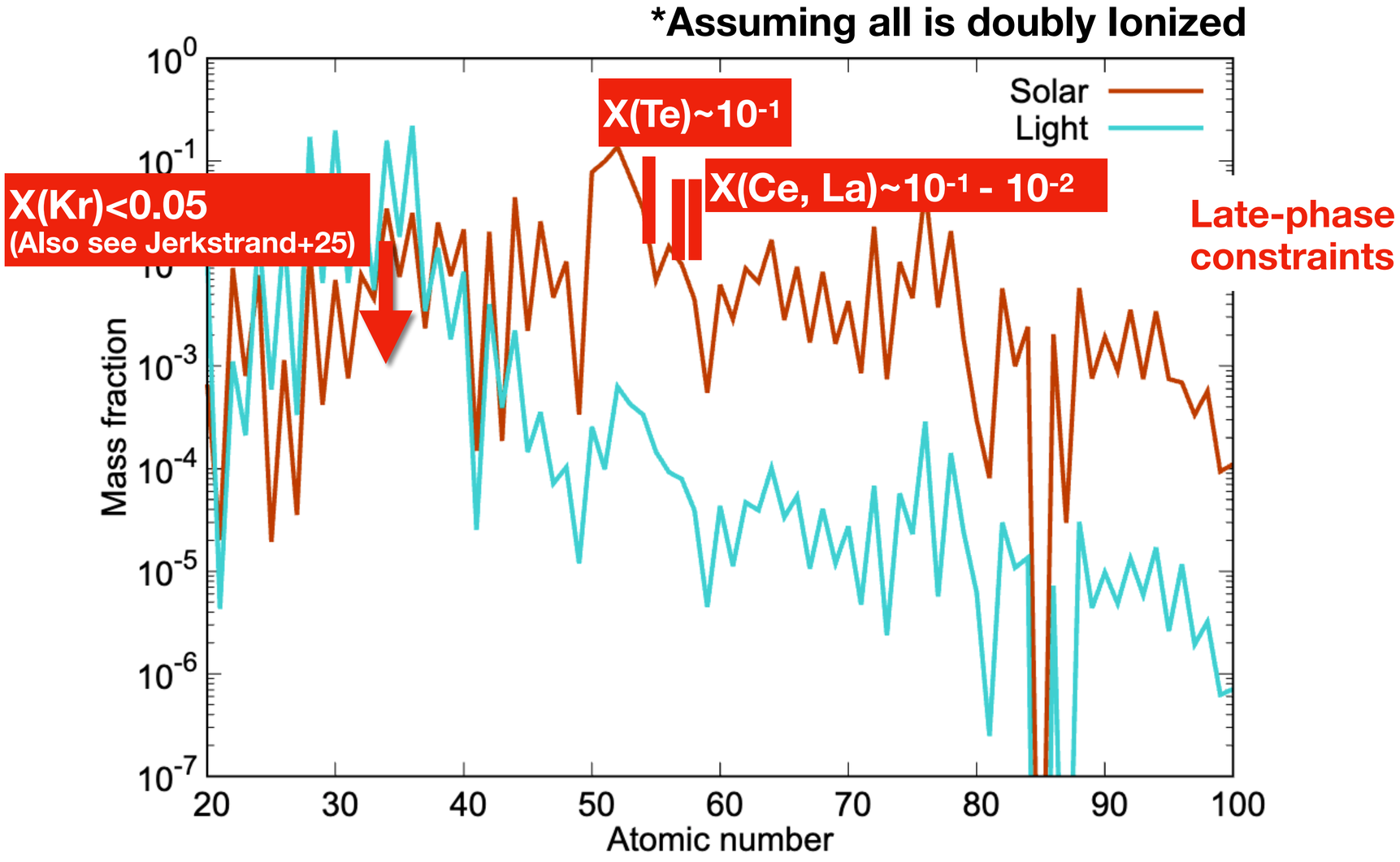

Nucleosynthesis Constraints

Good, but what about the continuum?

If the radiation field is coming from an inner optically thick region, allowed (E1) transitions can be caused by two mechanisms

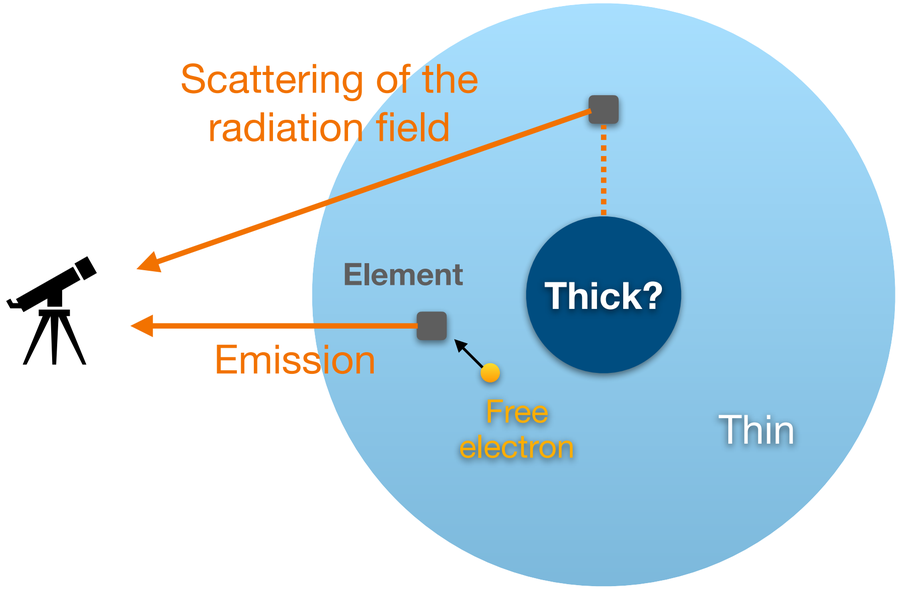

→ La III and Ce III become optically thick at ~ 10^{-3}

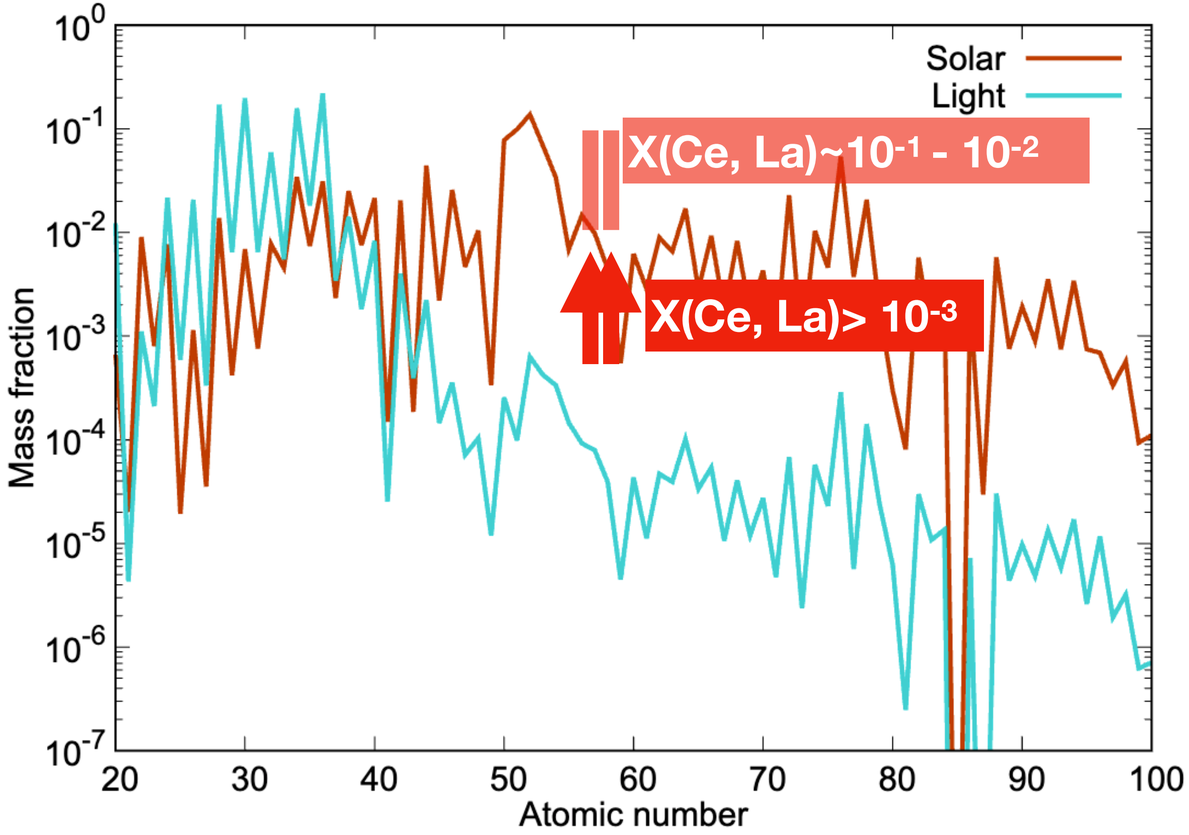

Nucleosynthesis Constraints

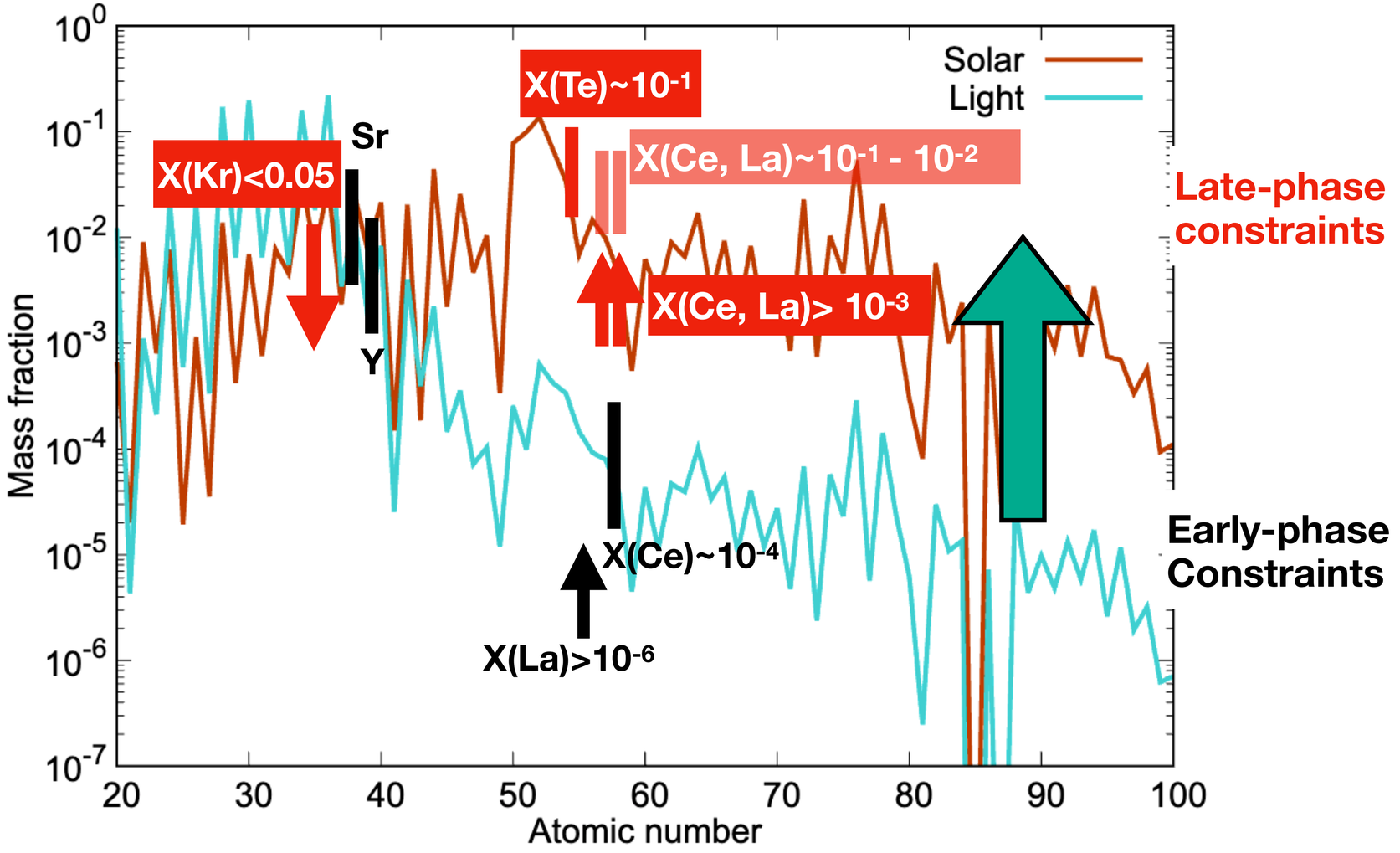

Mass fraction inferred for heavy elements is higher at late time

Discussion

Why different abundance distributions are needed to explain different epochs?

Early phase:

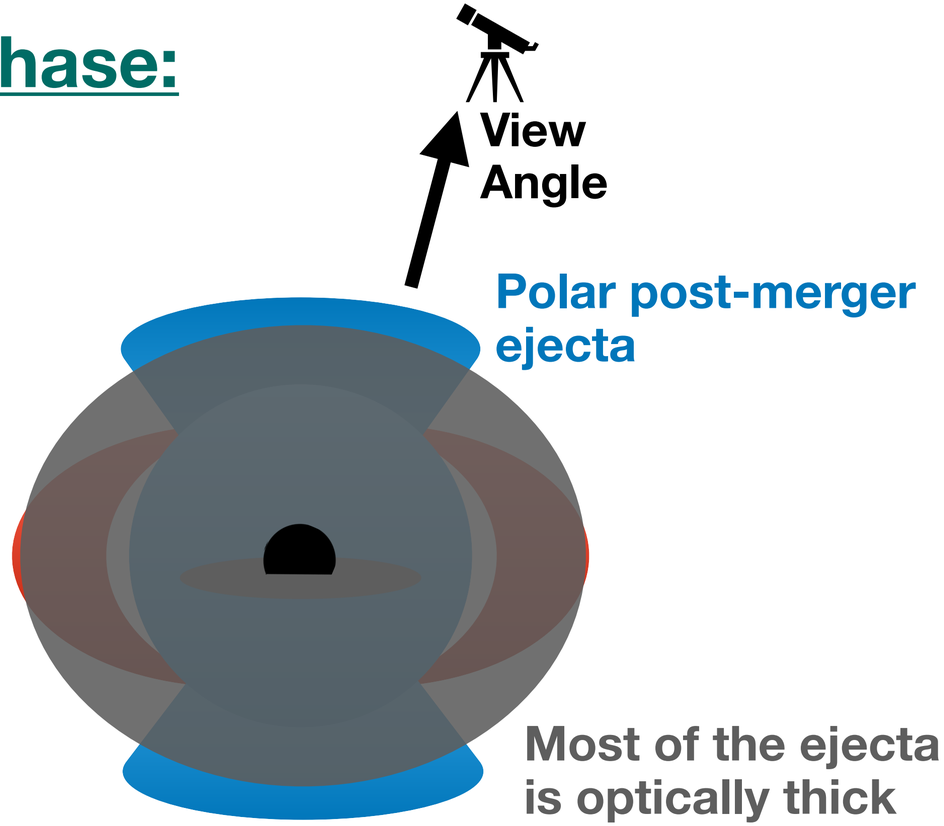

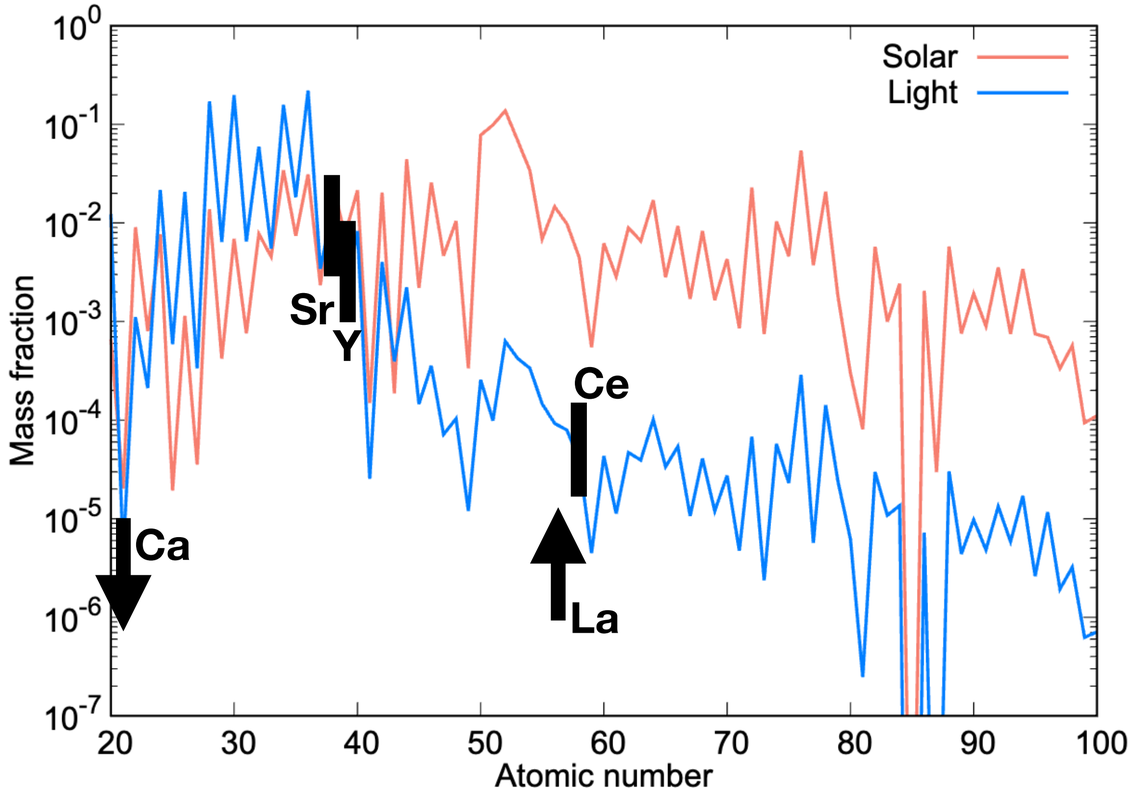

Absorption features appear due to elements along line of sight in the polar region

→ **Lower inferred mass fraction**

Discussion

Why different abundance distributions are needed to explain different epochs?

Late phase:

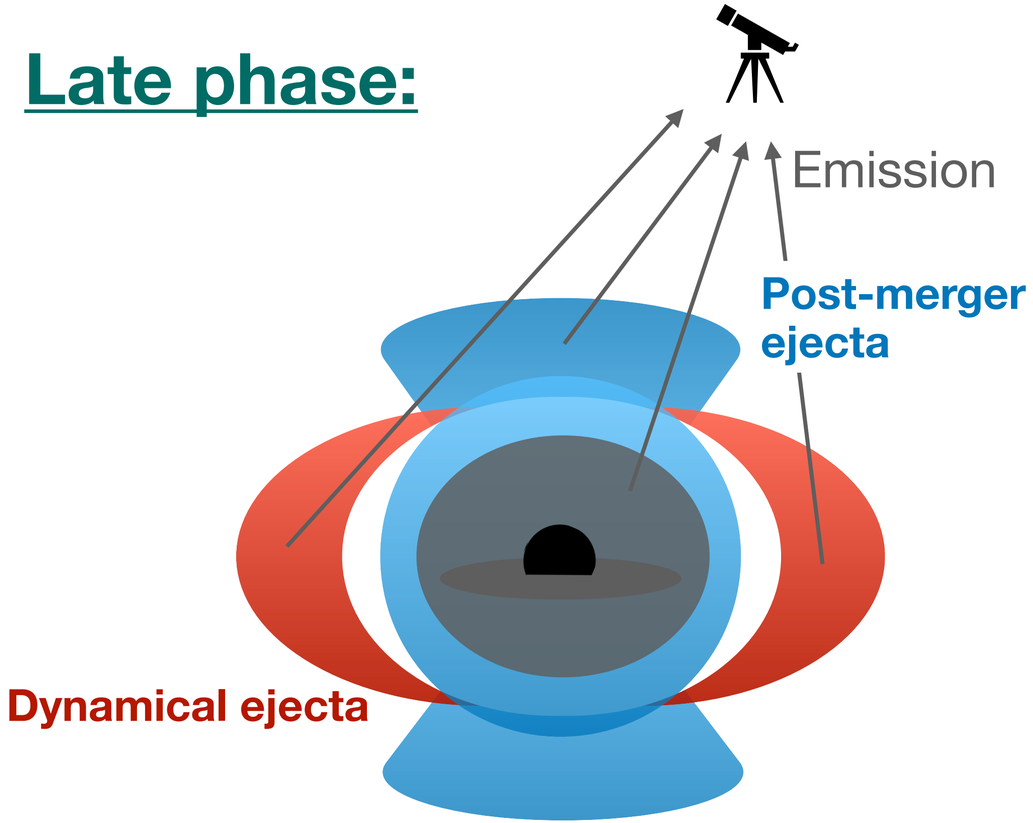

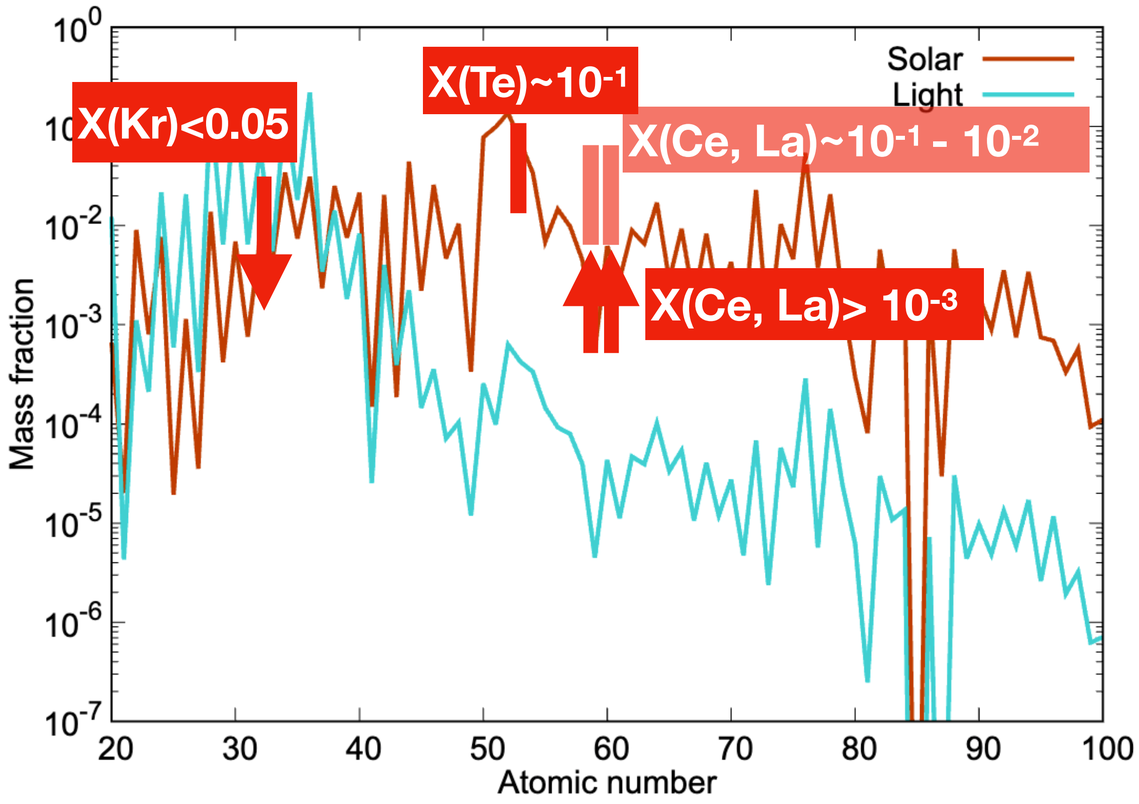

Most of the ejecta is optically thin and emission from different parts is observed

Mass fraction inferred reflects the overall synthesized matter in the merger

GW170817 nucleosynthesis is more consistent with solar r-process!

Summary

- **La III**, **Ce III**, and **Te III** as main contributors to three late-phase features
- Late phase estimates reflect the overall ejecta abundance
- Nucleosynthesis of heavy elements in GW170817 is **consistent with solar r-process abundance**

Selected Transitions

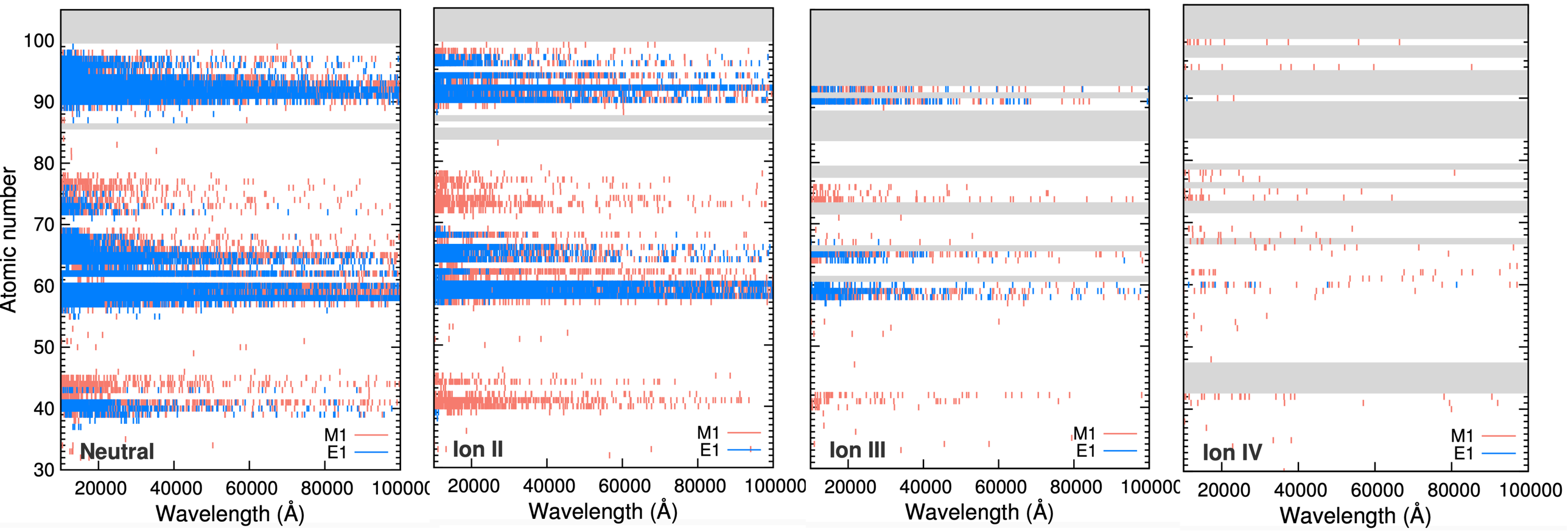

Abundance distributions used compared with the solar r-process residuals

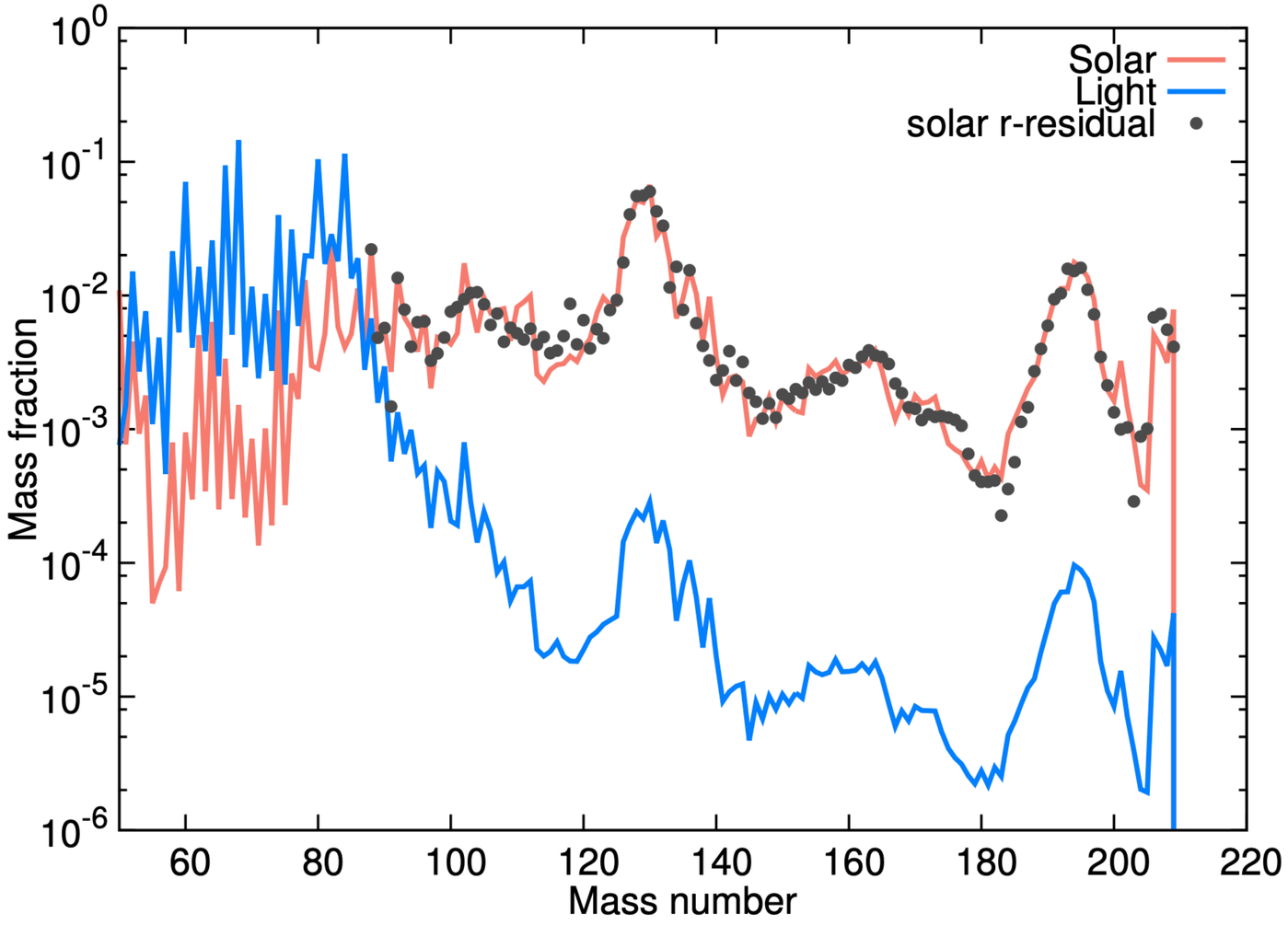

Atomic properties estimates

$n_{cr} < n_e$ (M1 transitions)

$$L = \Delta E\, n_X \frac{g_2}{\sum_k g_k e^{-\Delta E_k/kT}} e^{-E_2/kT} A_{2\to1}$$

For fine-structure:

$$A_{2\to1} = 1.3\ \mathrm{s}^{-1} \left(\frac{\lambda}{4\,\mu\mathrm{m}}\right)^{-3} f(J,L,S)$$

Where

$$f(L,S,J) = \frac{(J^2-(L-S)^2)((L+S+1)^2-J^2)}{12J(2J+1)} \quad \text{if } J_u = J_l + 1$$

$$f(L,S,J) = \frac{((J+1)^2-(L-S)^2)((L+S+1)^2-(J+1)^2)}{12(J+1)(2J+1)} \quad \text{if } J_u = J_l + 1$$

Pasternack (1940)

Other M1 transitions: $A_{2\to1} = 1$

$n_{cr} > n_e$ (E1 transitions and a few M1)

$$L = \Delta E\, n_X \frac{g_1}{\sum_k g_k e^{-\Delta E_k/kT}} e^{-E_1/kT} q_{2\to1}$$

$$q_{1\to2} = \frac{8.629\times10^{-6}}{T^{1/2}} \frac{\Upsilon_{1\to2}}{g_1} \exp(-\Delta E/kT)$$

Where $\Upsilon_{2\to1} = \int_0^\infty \Omega_{2\to1} e^{-E/kT} d\left(\frac{E}{kT}\right)$

Calibrated theoretical calculations by Flörs+25

For E1:

$$\Omega_{2\to1} = 2.388\,\bar{G} \left(\frac{\lambda}{1\mu m}\right)^3 \left(\frac{g_2 A_{2\to1}}{10^6\ \mathrm{s}^{-1}}\right)$$

Van Regemorter (1962)

For M1, we assume a typical $\Omega_{2\to1} = 1$

Nucleosynthesis Constraints

Good, but what about the radiation field?

If the radiation field is coming from an inner optically thick region, allowed (E1) transitions can be caused by two mechanisms

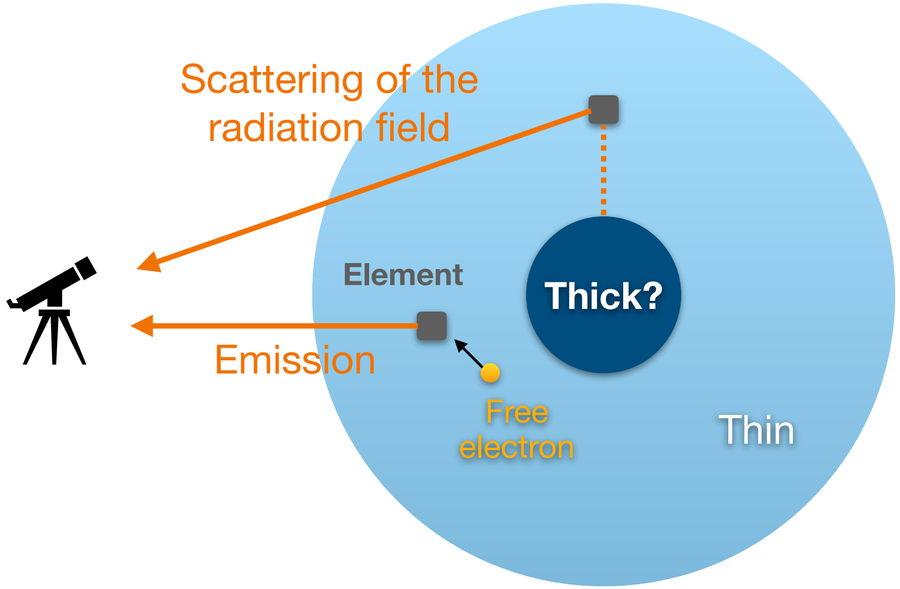

→ La III and Ce III should show P-Cygni features if optically thick

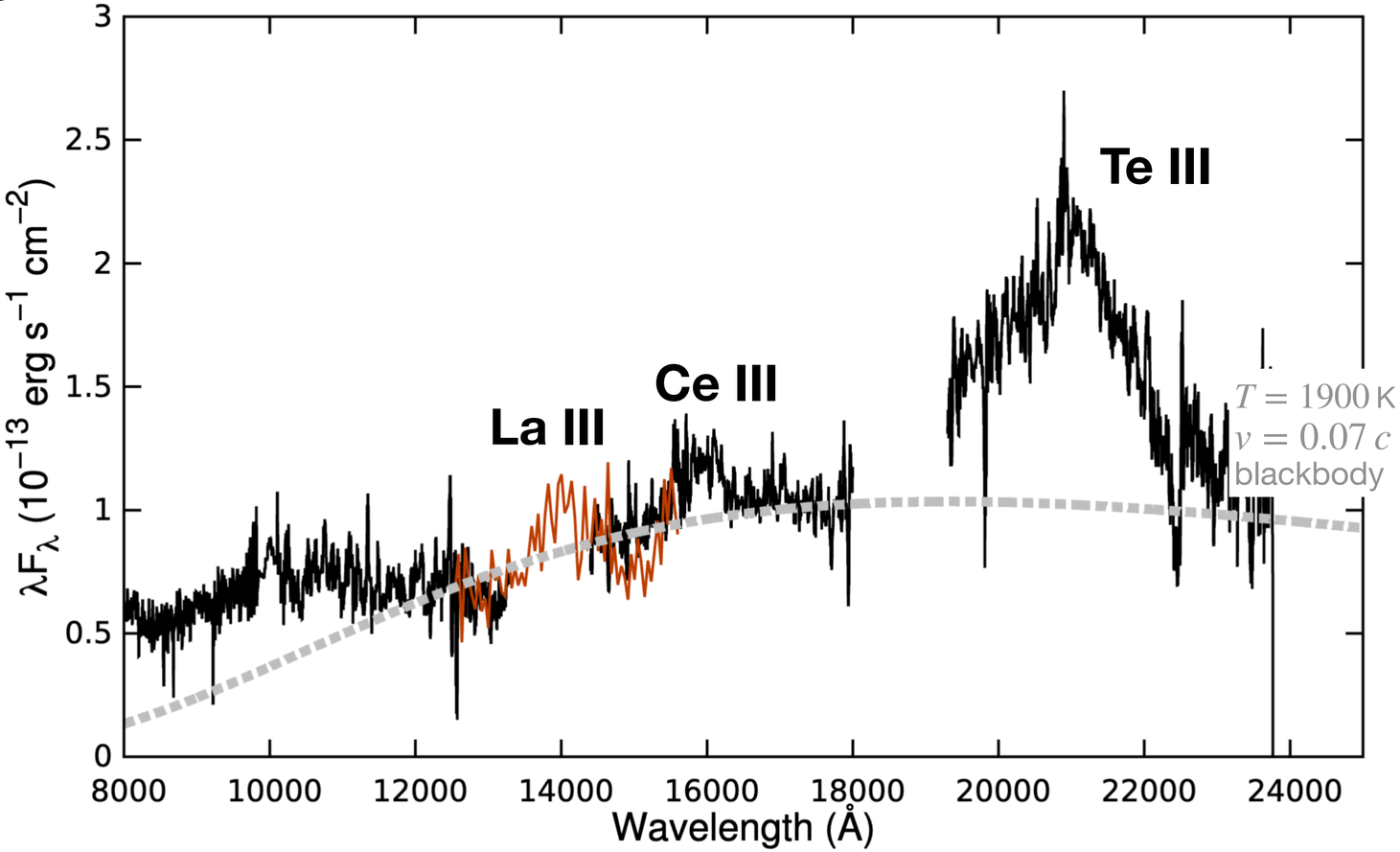

Are La III and Ce III optically thick?

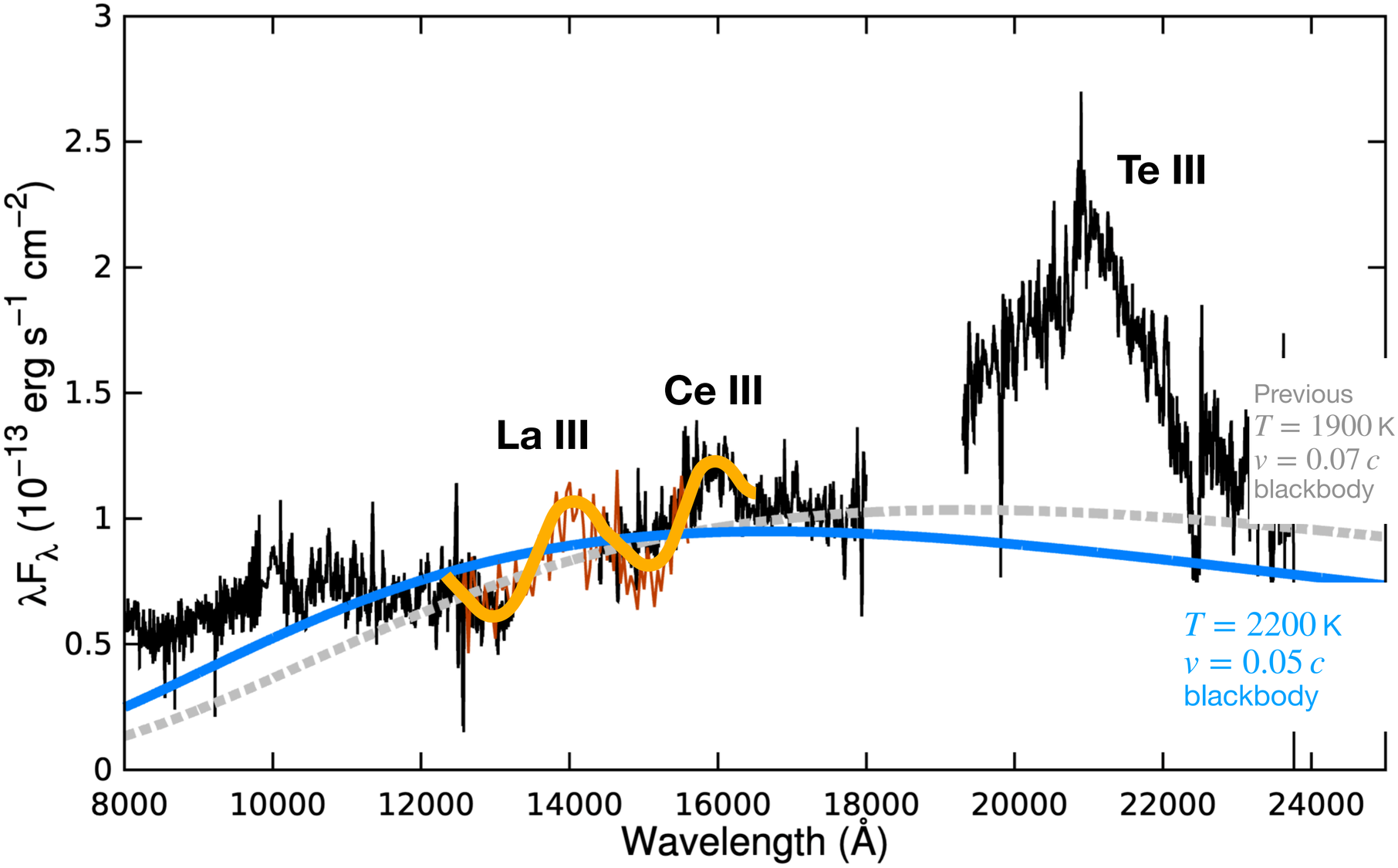

Nucleosynthesis Constraints

Sobolev optical depth of Ce III and La III as a function of their mass fractions

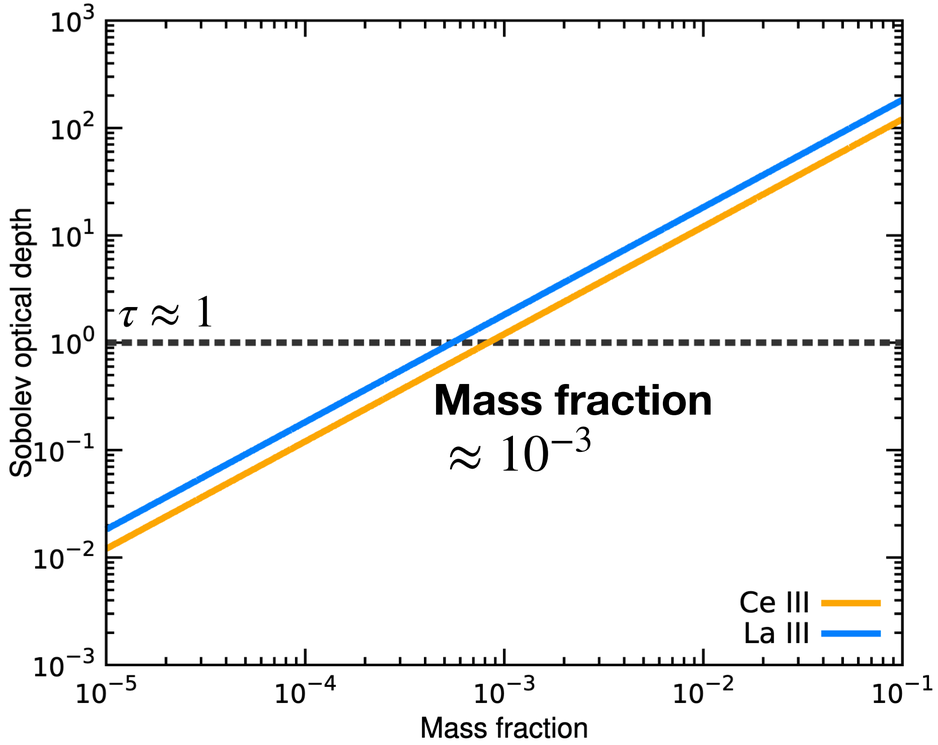

Transition is optically thick if $\tau \approx 1$

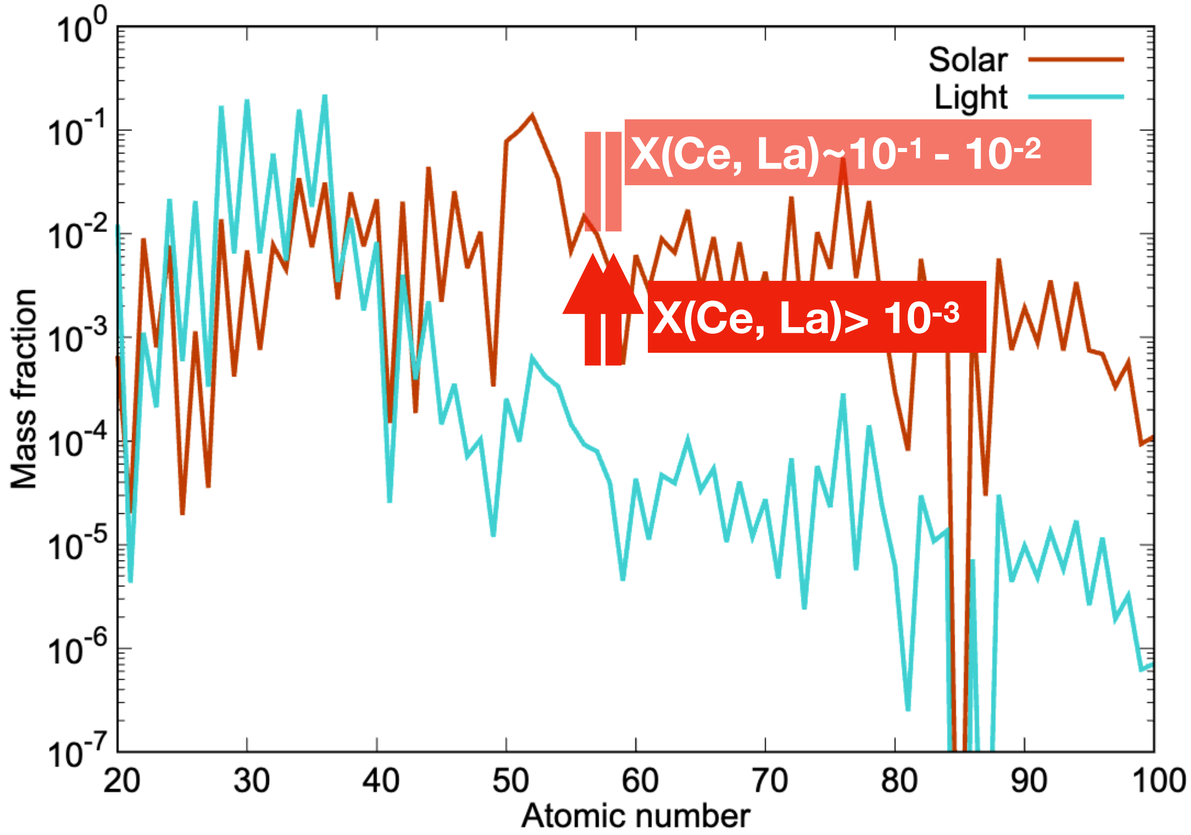

c.f. Sobolev optical depth

$$\tau = \frac{\pi e^2}{m_e c} n_{i,j}\, t\, \lambda\, g f\, \frac{1}{\Sigma}\, e^{-\frac{E_l}{kT}}$$

Models and Spectrum Comparison: light abundance

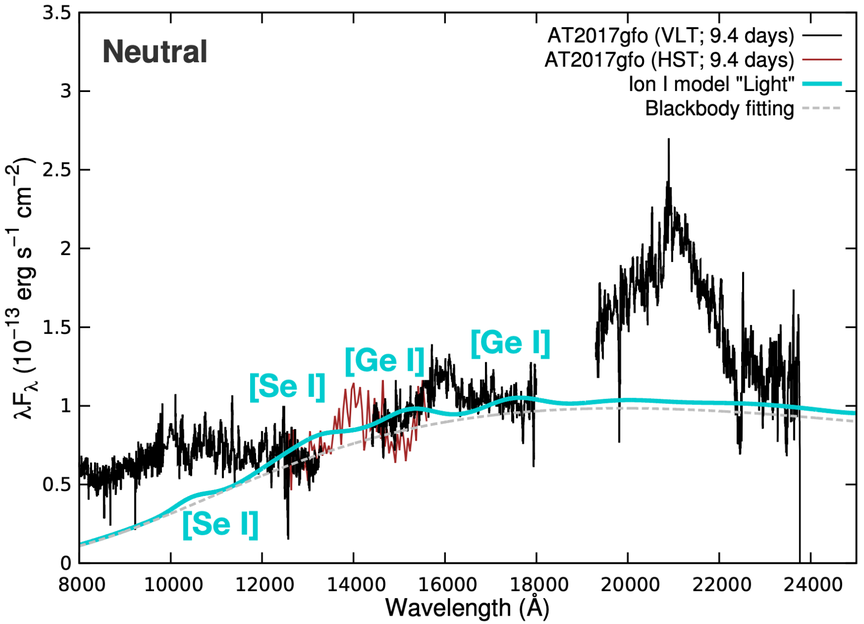

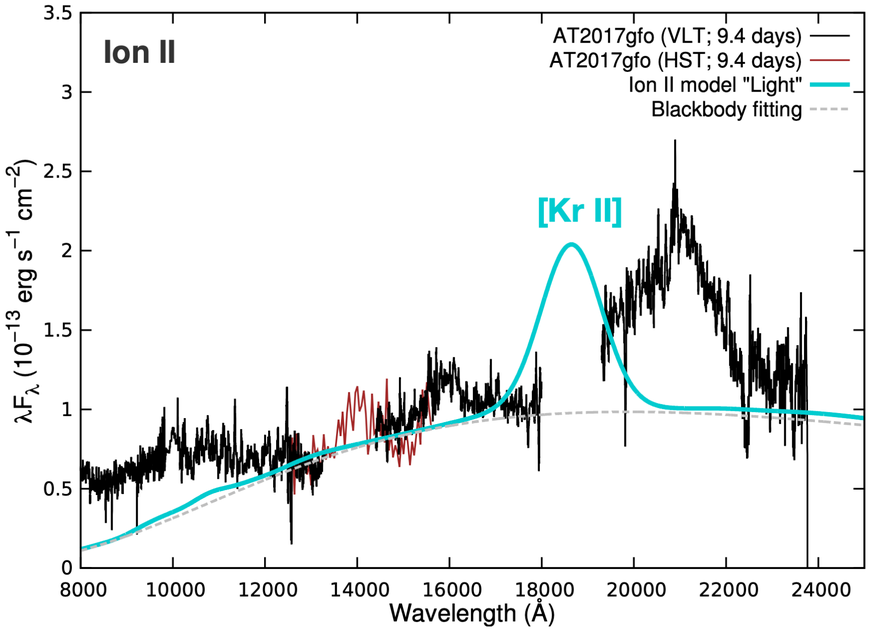

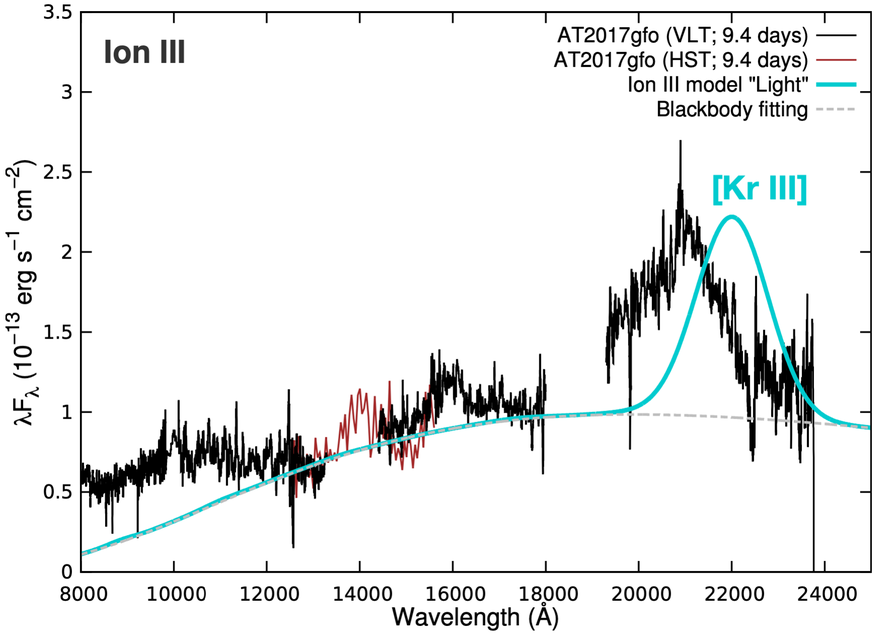

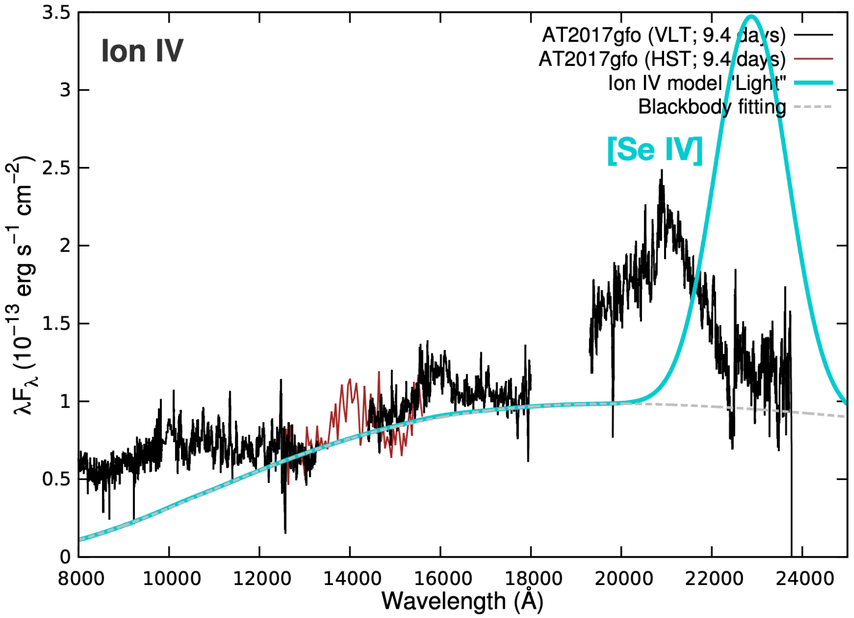

Models and Spectrum Comparison: solar abundance

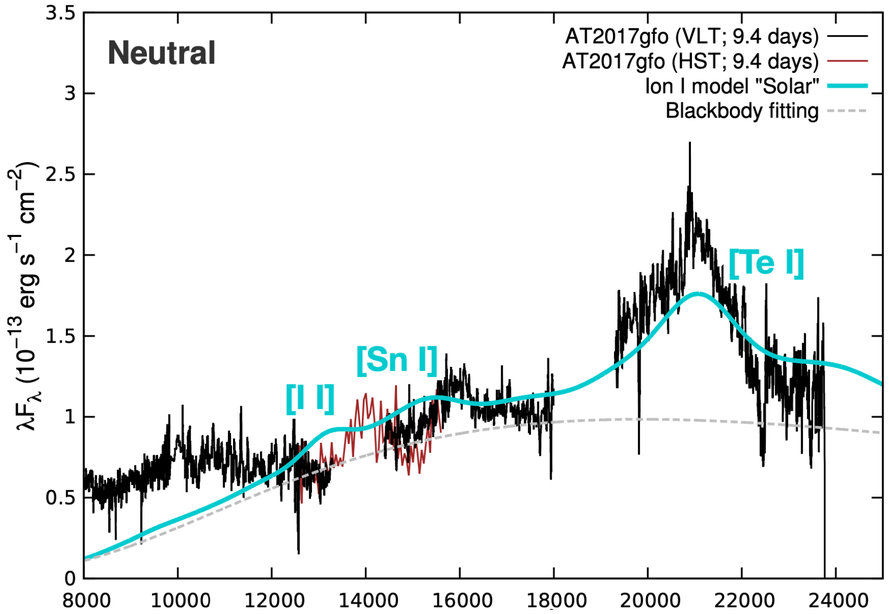

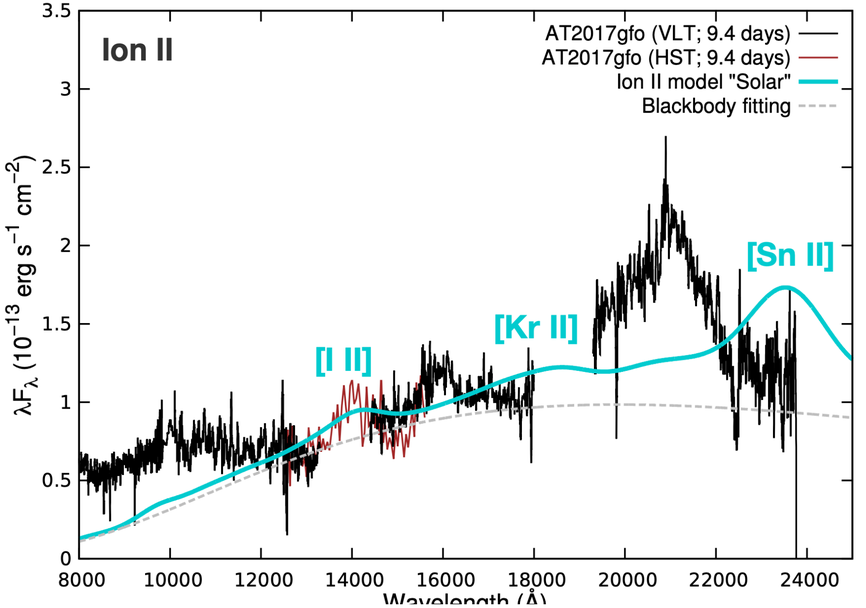

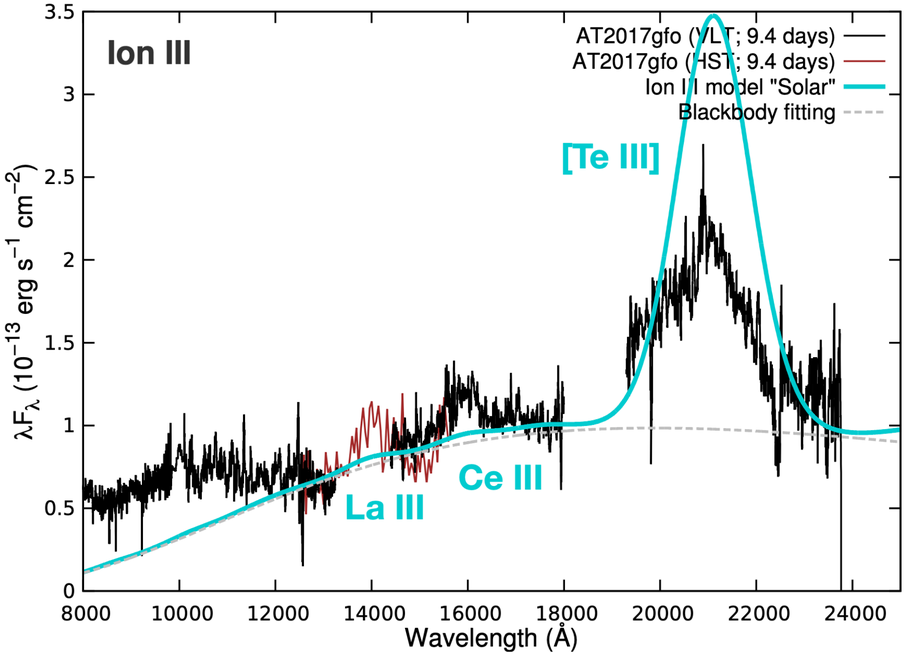

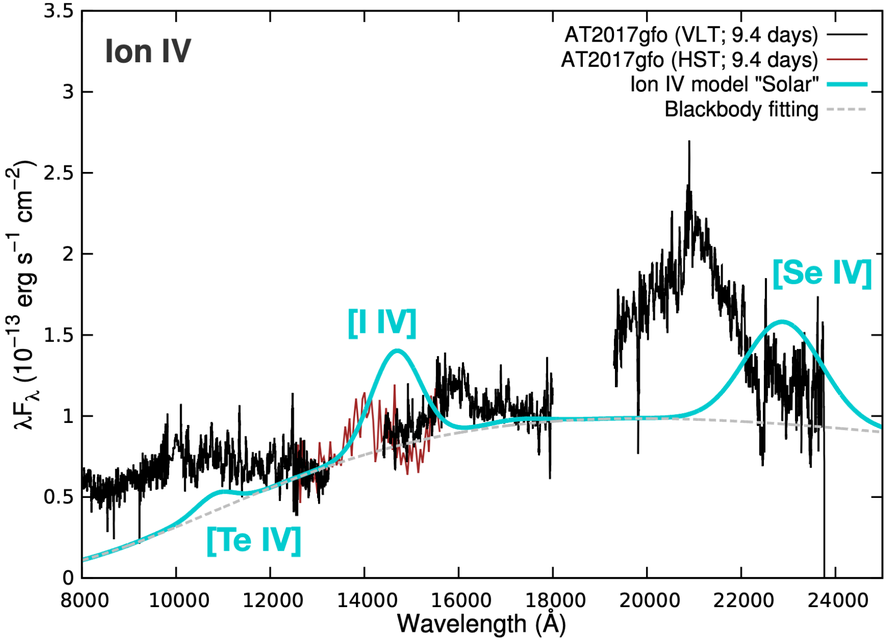

Gaussian Fitting best-fit parameters

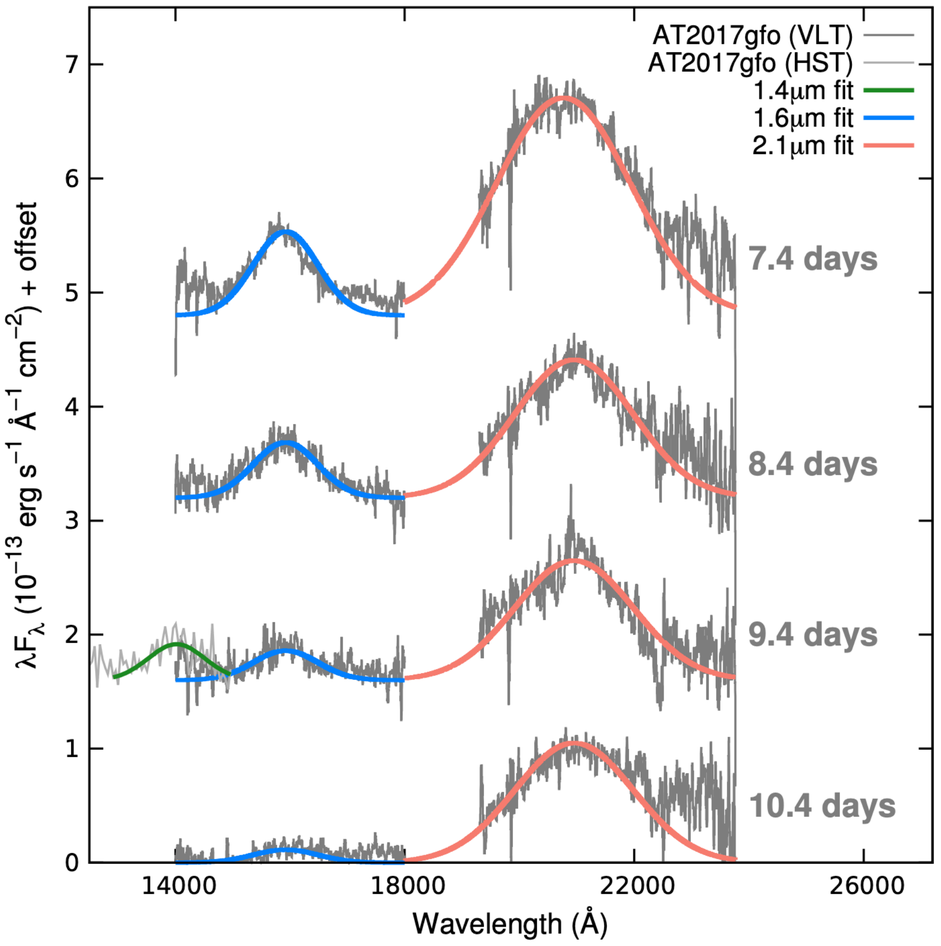

Feature	$\lambda_{\rm peak}$(Å)	$v_{\rm FWHM}$	Luminosity (erg s^{-1})
		7.4 days	
1.6 μm	15900	0.12 c	1.26×10^{39}
2.1 μm	20700	0.24 c	4.89×10^{39}
		8.4 days	
1.6 μm	15900	0.12 c	8.11×10^{38}
2.1 μm	20900	0.16 c	2.87×10^{39}
		9.4 days	
1.4 μm	14000	0.12 c	5.40×10^{38}
1.6 μm	15900	0.12 c	4.44×10^{38}
2.1 μm	20900	0.16 c	2.50×10^{39}
		10.4 days	
1.6 μm	15900	0.12 c	1.93×10^{38}
2.1 μm	20900	0.16 c	2.4×10^{39}

Required mass fraction fro Ce, La, and Te

Ce III feature is due to three lines

$$L = \Delta E_{1.59} n_e \frac{g_l}{\sum_k g_k e^{-E_k/kT}} \frac{X_{Ce} M_{ej}}{A_{Ce} m_u} \frac{8.6\times10^{-6}}{\sqrt{T}} \frac{\Upsilon_{1.59}}{g_l} e^{-\Delta E_{1.59}/kT}$$

$$+\Delta E_{1.58} n_e \frac{g_l e^{-E_l/kT}}{\sum_k g_k e^{-E_k/kT}} \frac{X_{Ce} M_{ej}}{A_{Ce} m_u} \frac{8.6\times10^{-6}}{\sqrt{T}} \frac{\Upsilon_{1.58}}{g_l} e^{-\Delta E_{1.58}/kT}$$

$$+\Delta E_{1.61} n_e \frac{g_l e^{-E_l/kT}}{\sum_k g_k e^{-E_k/kT}} \frac{X_{Ce} M_{ej}}{A_{Ce} m_u} \frac{8.6\times10^{-6}}{\sqrt{T}} \frac{\Upsilon_{1.61}}{g_l} e^{-\Delta E_{1.61}/kT}$$

La III feature is due to two line

$$L = \Delta E_{1.38} n_e \frac{g_l}{\sum_k g_k e^{-E_k/kT}} \frac{X_{La} M_{ej}}{A_{La} m_u} \frac{8.6\times10^{-6}}{\sqrt{T}} \frac{\Upsilon_{1.38}}{g_l} e^{-\Delta E_{1.38}/kT}$$

$$+\Delta E_{1.41} n_e \frac{g_l}{\sum_k g_k e^{-E_k/kT}} \frac{X_{La} M_{ej}}{A_{La} m_u} \frac{8.6\times10^{-6}}{\sqrt{T}} \frac{\Upsilon_{1.41}}{g_l} e^{-\Delta E_{1.41}/kT}$$

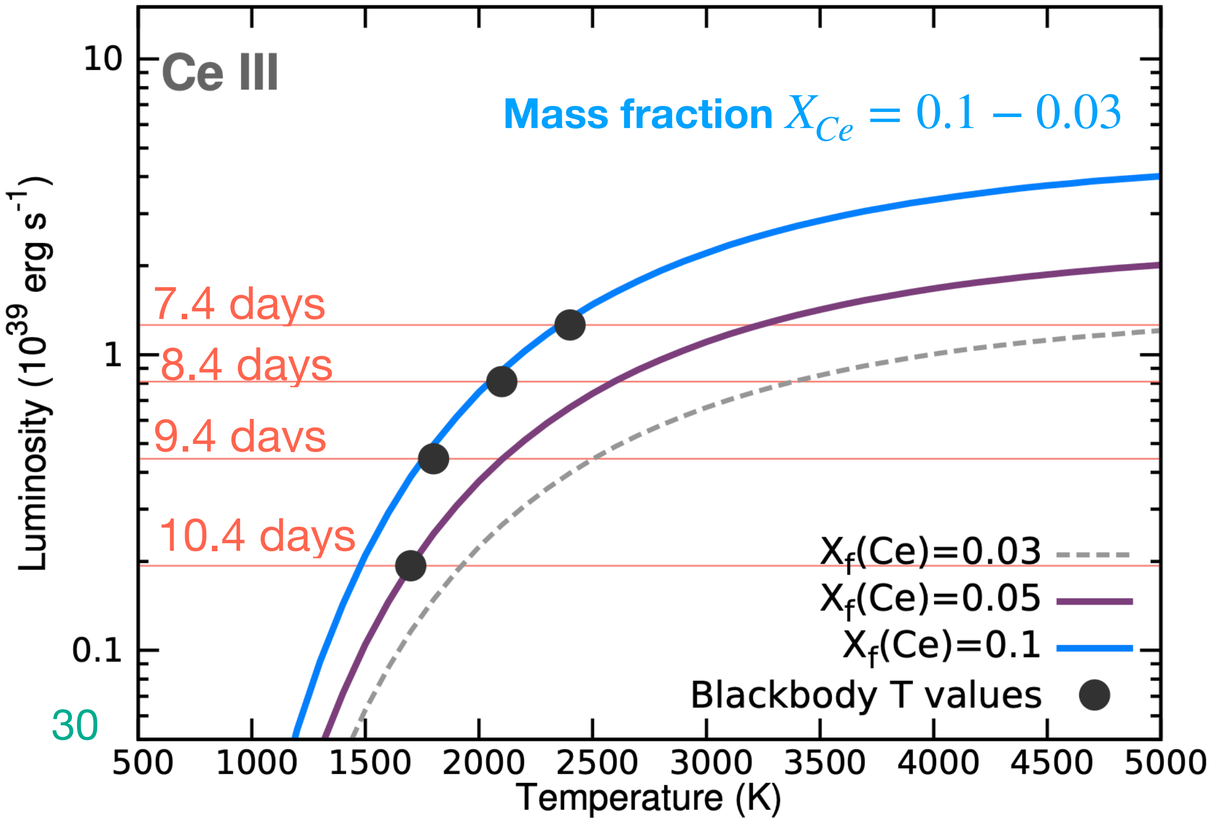

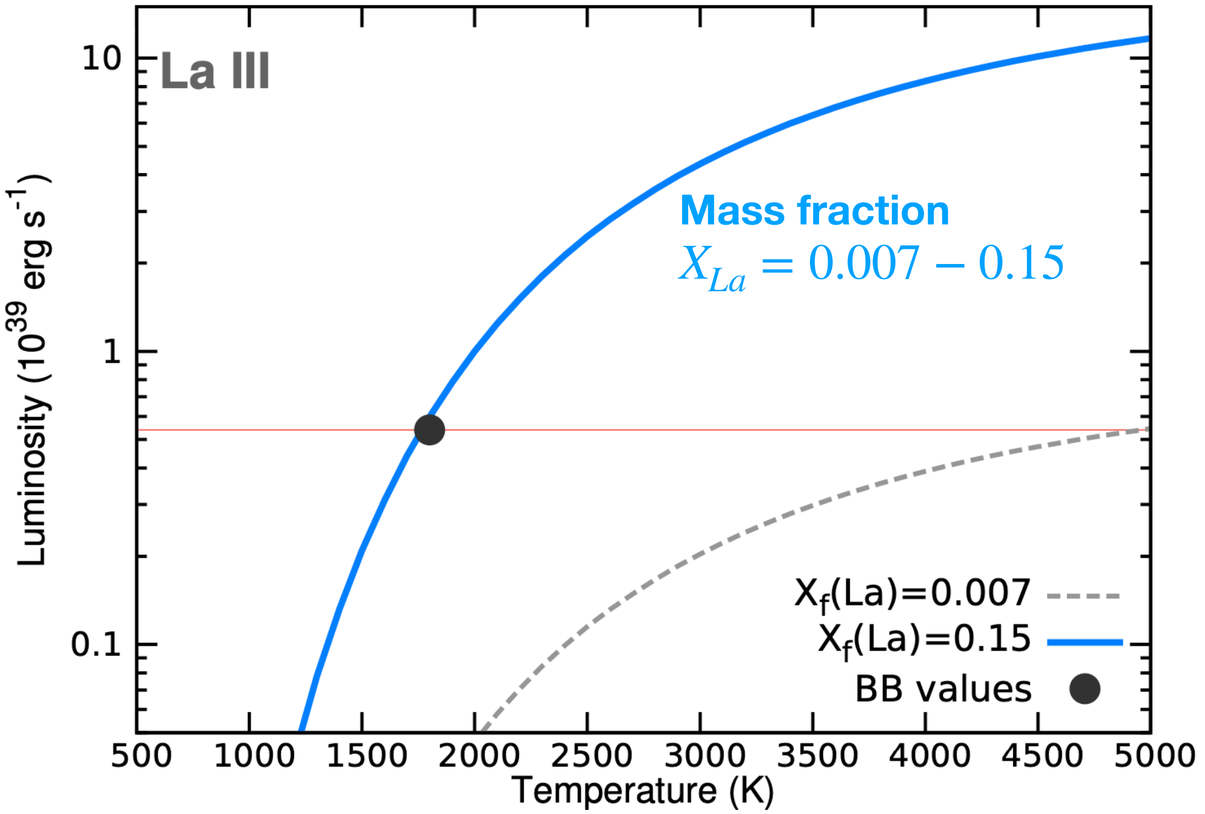

Required mass fraction fro Ce, La, and Te

Te III feature is due to one line

$$L = \Delta E_{2.1} n_e \frac{g_l}{\sum_k g_k e^{-E_k/kT}} \frac{X_{Te} M_{ej}}{A_{Te} m_u} \frac{8.6 \times 10^{-6}}{\sqrt{T}} \frac{\Upsilon_{2.1}}{g_l} e^{-\Delta E_{2.1}/kT}$$

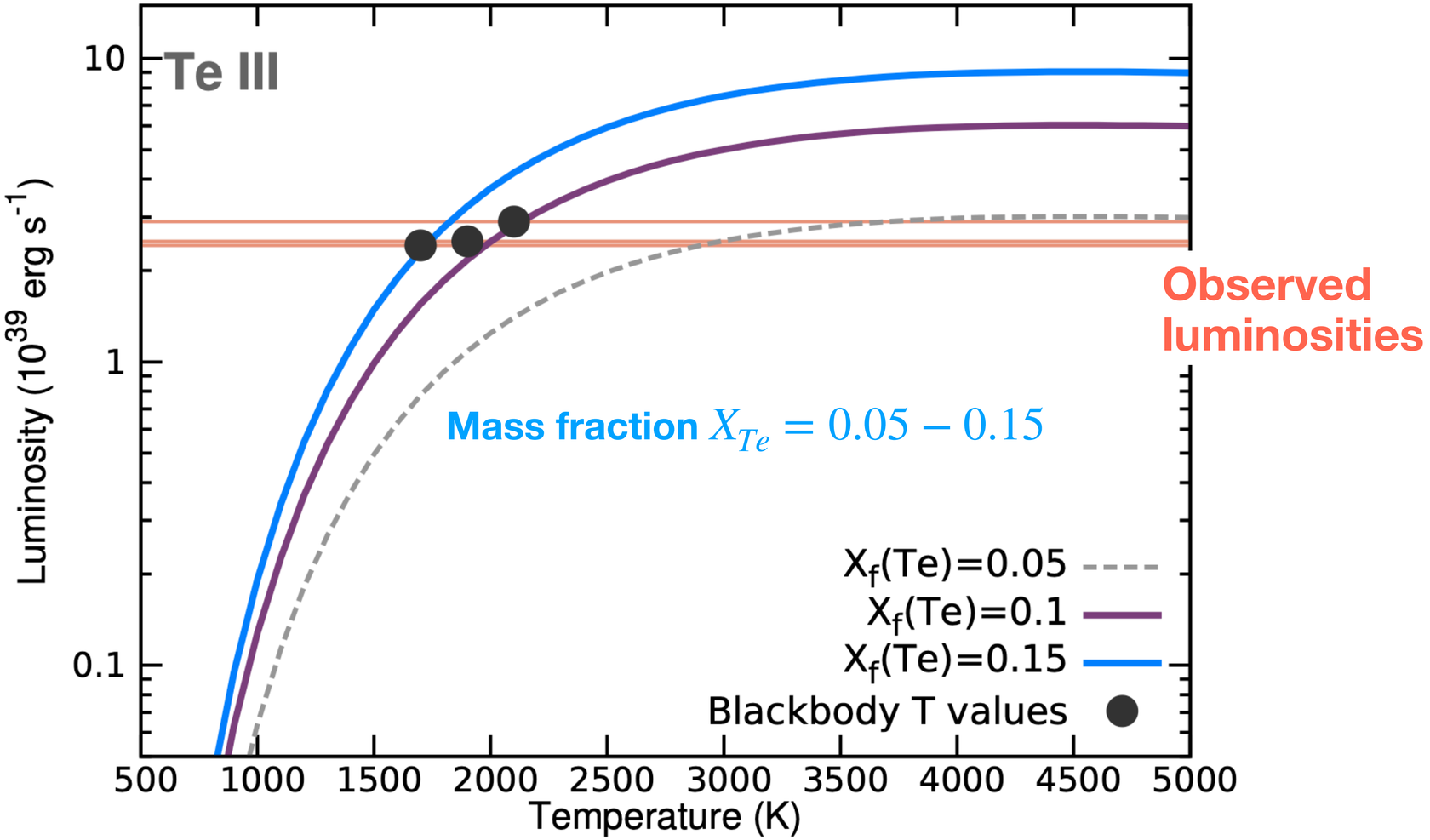

Observed luminosities

Important Candidates (2.1 feature)

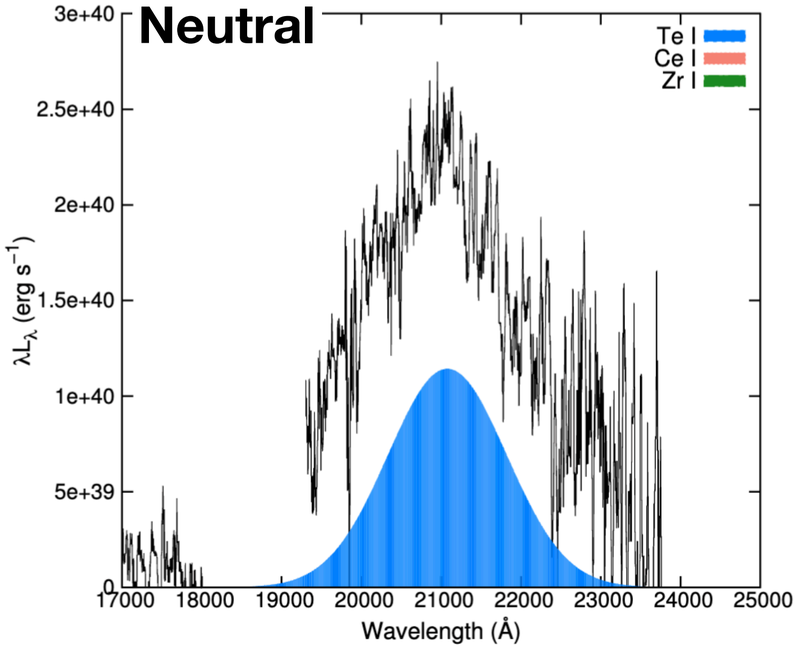

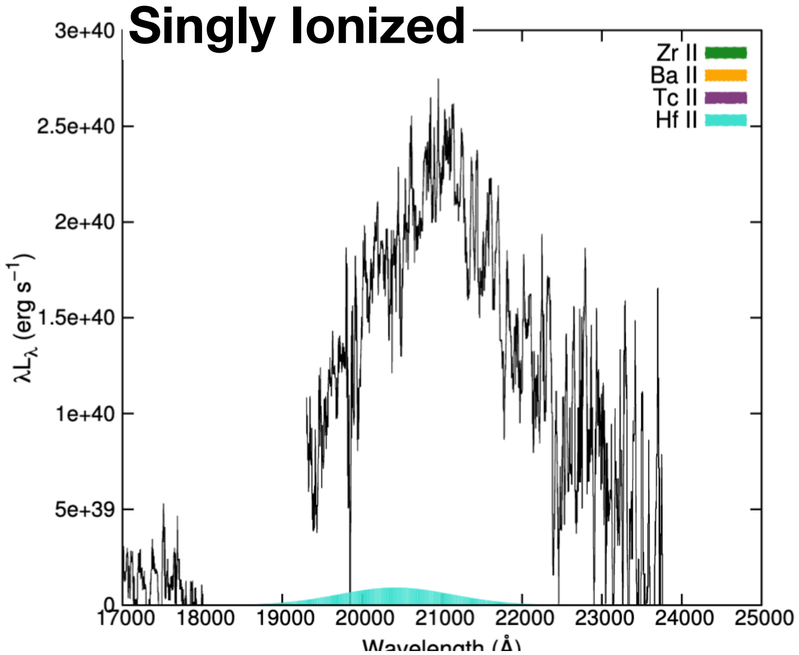

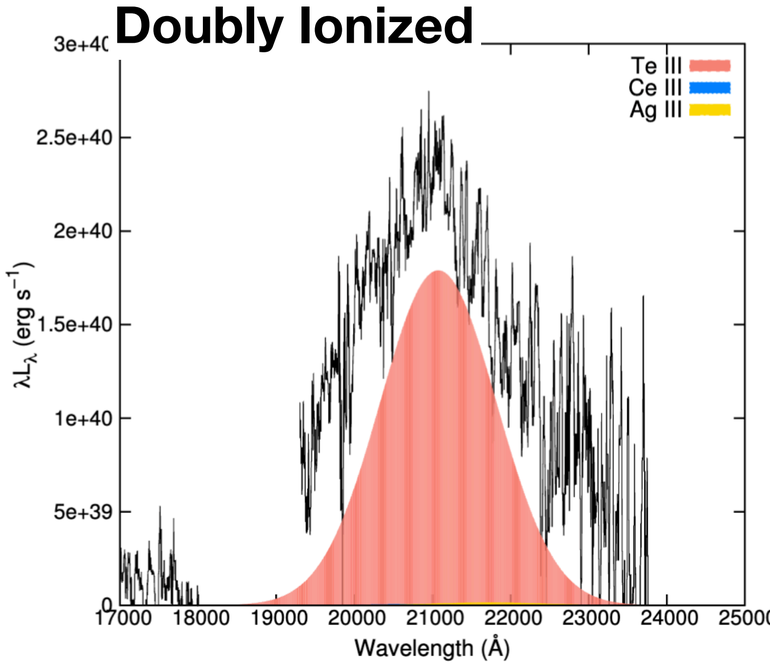

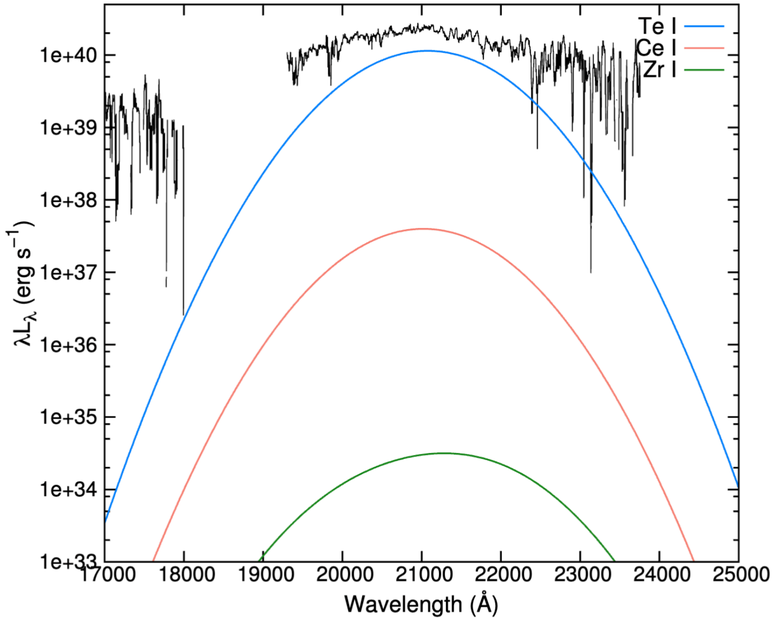

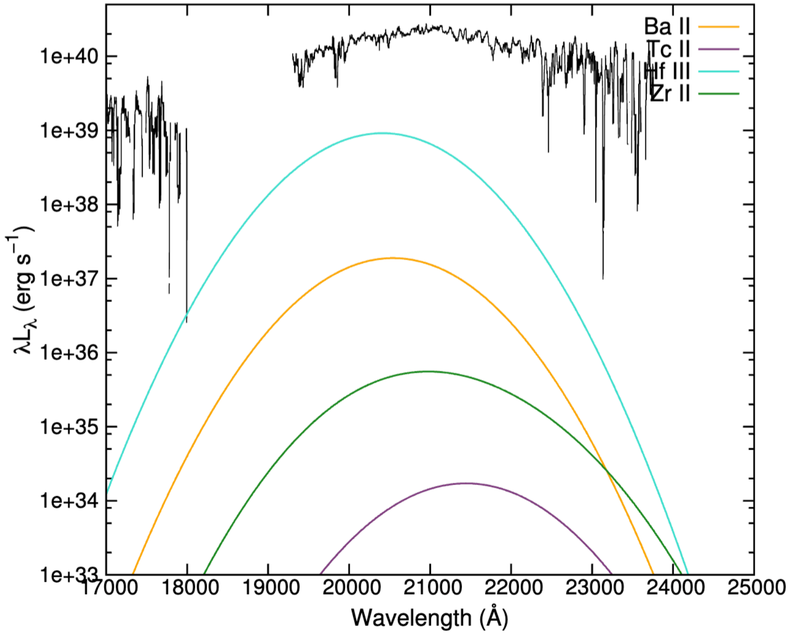

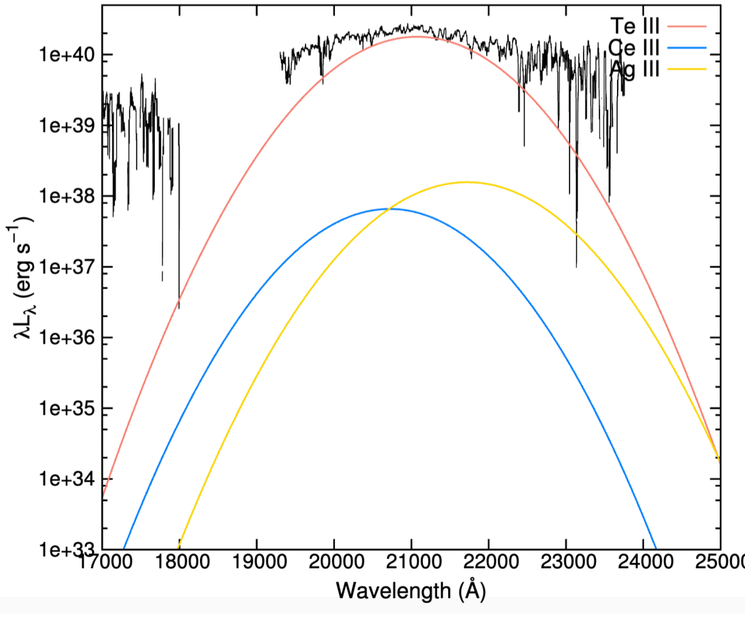

Important Candidates for 2.1 feature (Atomic data)

Element	Wavelength	Lower energy	Computed luminosity (erg/s)	Energy-average collision strength	A-value
Te I	21048	0.0	1.0E+39	1.16	6.00
Ce I	20691	0.0	3.5E+36	13.05	5.58E+08
Zr I	20531	0.0	9.6E+32	0.45	5.2E-05
	21373	0.0	7.4E+32	1.64	1.8E-05
	21514	0.07	1.6E+33	2.89	1.4E-04
Ba II	20517	0.0	1.7E+37	2.7	0.79
Zr II	20657	0.35	2.4E+34	1.17	1.16E-02
	21014	0.41	1.9E+34	0.16	1.14E-02
	21656	0.35	1.3E+34	0.107	6.1E-03
Tc II	21416	0.0	1.5E+33	0.16	3.98E-03
Te III	21048	0.0	1.6E+39	1.5	5.8
Ag III	21695	0.0	1.4E+37	0.4	7.4
Ce III	20691	0.19	5.7E+36	1.34	4.7E+04